Factors influencing storm-generated suspended-sediment concentrations and loads in four basins of contrasting land use, humid-tropical Puerto Rico

A.C. Gellis *

U.S. Geological Survey, Maryland Water Science Center, 5522 Research Park Drive, Baltimore, MD 21228, United States

ABSTRACT

The significant characteristics controlling the variability in storm-generated suspended-sediment loads and concentrations were analyzed for four basins of differing land use (forest, pasture, cropland, and urbanizing) in humid-tropical Puerto Rico. Statistical analysis involved stepwise regression on factor scores. The explanatory variables were attributes of flow, hydrograph peaks, and rainfall, categorized into 5 flow periods: (1) the current storm hydrograph, (2) the flow and rainfall since the previous storm event, (3) the previous storm event, (4) 2nd previous storm event, and (5) the 3rd previous storm event. The response variables (storm generated sediment loads and concentrations) were analyzed for three portions of the storm hydrograph: (1) the entire storm, (2) the rising limb, and (3) the recessional limb. Hysteresis differences in sediment concentration between the rising and falling limb were also analyzed using these explanatory variables.

Sediment availability in the study basins is related to land use and underlying geology. The supply of sediment and its location in the watershed have a strong influence on how current and previous storm events, and flow and rainfall between storm events, affect sediment loads and concentrations. In basins with limited sediment availability (forest and pasture), previous storm events supply sediment to the channel. This in-channel sediment becomes the source of sediment on the rising limb of the next event and clockwise hysteresis occurs. In the cropland basin with high sediment availability, sediment delivered to the channel during events becomes the source of sediment on the rising limb of the next event and clockwise hysteresis occurs. In the urbanizing basin with high sediment availability, counterclockwise hysteresis is prevalent as stormwater runoff dilutes suspended-sediment concentrations on the rising limb and upland sediment arrives on the hydrograph recession. In the urbanized basin, previous storm events flush sediment from the system. The statistical approaches presented here can be used to generate hypotheses on the location and delivery of watershed sediment sources which can improve the design of appropriate field studies.

Published by Elsevier B.V.

1. Introduction

Suspended-sediment concentrations in many rivers vary by several orders of magnitude at a given discharge. The scatter is thought to be caused by a hysteresis where at the same discharge on the rising limb and falling limb of the hydrograph, suspended-sediment concentrations are either higher or lower (Goodwin and Denton, 1991; Kattan et al., 1987; Picouet et al., 2001; Sidle and Campbell, 1985; VanSickle and Beschta, 1983; Wang et al., 1998) (Fig. 1; Table 1). For most streams, the hysteresis is clockwise (TYPE-1 in Fig. 1), where higher suspended-sediment concentrations occur on the rising limb of the hydrograph and lower concentrations occur on the recessional limb (Glysson, 1987; Rieger and Olive, 1986; VanSickle and Beschta, 1983; Wood, 1977).

Causes for TYPE-1 hysteresis have been explained primarily by a first flush mechanism (Table 1), where during rising flow, readily

available sediment in channel storage is readily mobilized, causing a spike in sediment concentration to occur before peak discharge. Kurashige (1994) proposed that higher shear stress on the rising limb can lead to sediment mobilization of bed sediment and higher sediment concentrations. Exhaustion of sediment sources that occurs during the course of a runoff event can lead to reduced sediment concentrations on the recessional limb of the hydrograph and a TYPE-1 hysteresis (Kurashige, 1994). Causes for sediment exhaustion include decreased detachment of soil particles at the cessation of rainfall, dilution effects from increases in groundwater flow to the stream, and progressive wetting and armoring of soil (Walling and Webb, 1982) (Table 1). Seasonality is strongly linked to climate, which influences sediment availability and can control clockwise and counterclockwise hysteresis (Wang et al., 1998).

Counterclockwise hysteresis loops (TYPE-3 in Fig. 1) occur less frequently and have been explained by a delayed source from tributaries or due to bank collapse on the recessional limb of the hydrograph (Rinaldi et al., 2004; Simon et al., 2000) (Table 1). Heidel (1956) and Marcus (1989) explained TYPE-3 hysteresis as a hydraulic phenomenon

* Tel.: +1 443 498 5581; fax: +1 443 498 5510.
E-mail address: agellis@usgs.gov.
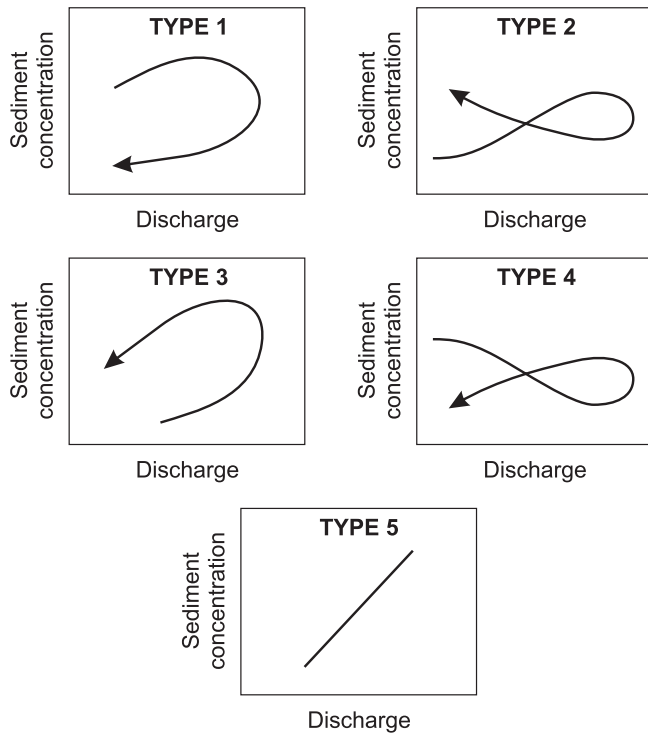
Fig. 1. Hysteresis types (after Williams, 1989; Kurashige, 1994). Arrows indicate direction through time. TYPE-1 clockwise, TYPE-2 figure eight, clockwise early in storm reversing to counterclockwise, TYPE-3 counterclockwise, TYPE-4 figure eight, counterclockwise early in storm reversing to clockwise, and TYPE-5 no exhaustion.

occurring in large rivers when the flood wave travels faster than the sediment wave (Table 1). Figure eight hysteresis loops (TYPE-2 and TYPE-4) can be caused by a variety of factors related to sediment sources and storm intensity (Table 1).

Several approaches have been used to understand the factors controlling the scatter of suspended-sediment concentrations, including statistical analysis of the relation of discharge to suspended-sediment concentrations (sediment-transport curves) (Walling and Webb, 1982),

nested sediment collection designs with bank erosion monitoring (Smith and Dragovich, 2009), and multivariate statistical analysis (Duvert et al., 2010; Guy, 1964; Walling, 1974). Walling (1974) analyzed the scatter in sediment-transport curves for a 0.26 km² watershed in Devon, England. Scatter was obvious in the sediment-transport curve, where discharge only accounted for 33% of the total variance in suspended-sediment concentration. Scatter in the sediment-transport curve was attributed to three factors: hysteresis, a decrease of sediment availability in multi-peaked events, and seasonality. Walling (1974) found that by using four variables to describe suspended-sediment concentration—(1) discharge, (2) rising or falling stage, (3) flow level at the beginning of an event, and the (4) shape of the hydrograph (index of flood intensity) —70% of the variation was explained; an improvement over the previous 33%. Guy (1964) analyzed the factors affecting storm-period sediment transport for seven streams in the Atlantic coastal area of the United States. The mean concentration of sediment for a storm event was regarded as a better response variable than sediment discharge. Water discharge proved to be the most important variable in describing sediment concentration. Sediment discharge was positively correlated with storm intensity, measured as the peakflow divided by total runoff (Guy, 1964).

The meteorological and hydrologic characteristics of previous storm events and characteristics between runoff events may influence suspended-sediment characteristics of the current event (Beschta, 1987; Duvert et al., 2010; Moore, 1984; Walling and Webb, 1982; Wood, 1977). Previous storms can either increase or exhaust the supply of sediment to the channel. If a previous runoff event was relatively high, sediment may have been flushed from hillslopes and the channel, and the suspended-sediment concentrations of the current event may be low (Walling and Webb, 1982). A sequence of events may further reduce sediment concentrations (Rodriguez-Blanco et al., 2010). The effects of previous storms may diminish as the time between events increases, a period referred to as the "recovery period" (Walling and Webb, 1982). In some basins, large storms may provide sediment to the channel that is transported in a subsequent storm event (Duvert et al., 2010). Physical and biological processes that occur between runoff events may increase the sediment available for transport (Walling and Webb, 1982). Light rains occurring between runoff events may erode and transport sediment from the hillslopes to low-order channels, to the main channel, and to flood plains, where it remains in storage until high flows of the next runoff event mobilize it.

Table 1
Summary of hysteresis types in the literature and their causes.

Hysteresis type	Cause of hysteresis shape	Reference
TYPE 1 (clockwise)	Mobilization followed by depletion of in-channel or nearby sediment sources	Walling (1974), Wood (1977), Costa (1977), Bull et al. (1995), Seeger et al. (2004), Smith and Dragovich (2009)
	Formation of armored layer before peak discharge	Williams (1989)
	Bank erosion	Smith and Dragovich (2009)
	Maximum shear stress on the bed appears before the peak	Kurashige (1994)
	Water depth and water slope increases before peak discharge	Kurashige (1994)
	Increased base flow after peak discharge leading to dilution of sediment concentration	Walling (1974), Costa (1977), Baca (2008)
	Seasonality, higher concentration early in the year followed by flushing and depletion of sediment	Sidle and Campbell (1985), Kattan et al. (1987), Wang et al. (1998), Asselman (1999), Picouet et al. (2001)
TYPE 2 (figure then counterclockwise	Ice breakup	Williams (1989)
	Initial sediment contribution from the streambed and its banks; a delayed contribution of sediment from subbasins	Eder et al. (2010)
Type 3 (counterclockwise)	Floodwave traveling faster than mean flow velocity	Marcus (1989), Williams (1989), Brasington and Richards (2000)
	High soil erodibility	Williams (1989)
	Bank erosion	Simon et al. (2000), Rinaldi et al. (2004)
	Distant sediment source	Loughran et al. (1986), Williams (1989), Baca (2008)
	Upstream tributaries	Asselman (1999)
	Seasonality, lower concentrations early in the year followed by increasing sediment concentrations	Sidle and Campbell (1985), Wang et al. (1998)
	Thin, exposed soil surfaces	Kurashige (1994)
TYPE 4 (figure eight) counterclockwise then clockwise	Occurs under extreme dry conditions	Seeger et al. (2004)
TYPE 5 (stationary)	Uninterrupted supply of sediment	Wood (1977), Williams (1989)

Suspended sediment can contribute substantially to water-quality and habitat impairments (Larsen et al., 2010). In Puerto Rico, the impact of suspended sediment on degrading coral reef habitats can be substantial (Larsen and Webb, 2009; Warne et al., 2005). The attenuation of light by suspended sediment and nutrients is the leading causes of habitat degradation in the United States' largest estuary, Chesapeake Bay (Gellis et al., 2009). Suspended sediment can act as a vector for a wide variety of organic and inorganic chemical constituents (Horowitz, 2008). Determining the impact of human disturbance(s) on the erosion, transport, and delivery of suspended sediment is important in understanding the effect of sediment as a pollutant and its role in degraded aquatic habitats as well as developing tools to control sediment transport. With the exception of Douglas and Guyot (2004) analysis of streams in Malaysia, few studies have examined the characteristics of suspended-sediment transport in tropical rivers, specifically identifying causes for the variability in storm-generated suspended-sediment concentrations and loads. In part, this deficit is due to the lack of an extensive and accurate dataset from a humid-tropical region (Krishnaswamy et al., 2001).

The objectives of this study were to examine the hydrologic factors controlling storm-generated suspended-sediment loads and concentrations for four basins in humid-tropical Puerto Rico. Based on previous work in Puerto Rico it has been shown that sediment availability relates to ground cover through land use (Gellis et al., 1999). The four basins have differing land uses, ranging from the less available sediment in forested (Rio Icacos) and pasture (Quebrada Blanca) basins, to basins with greater sediment availability—the agricultural (Rio Caguitas) basin, and the urbanizing (Rio Piedras) basin. Thus, another objective of the study was to determine if differences in sediment availability between basins influence storm-generated suspended-sediment characteristics assuming that land use exerts an important control on sediment availability.

1.1. Previous studies in Puerto Rico

Sediment discharge and sediment yield vary regionally across Puerto Rico in response to natural and anthropogenic factors (Gellis et al., 2006; Larsen and Santiago-Roman, 2001; Larsen and Simon, 1993; Larsen and Stallard, 2000; Warne et al., 2005). Natural factors include deeply weathered soils and intense rainfall events that contribute to a wide variety of mass movements, including soil creep (Lewis, 1974), and landsliding (Jibson, 1989; Larsen and Santiago-Roman, 2001; Larsen and Simon, 1993; Larsen and Torres-Sanchez, 1992; Simon et al., 1990). In Puerto Rico, as in other areas of the world, land use is an important factor controlling soil erosion and suspended-sediment transport (Dunne, 1979; Gellis et al., 1999, 2006; Hooke, 2000; Krishnaswamy et al., 2001; Leopold, 1956; Sidle et al., 2006; Syvitski and Kettner, 2011). Results of statistical analyses on factors controlling annual sediment yields and annual sediment concentrations for 12 sub-basins of the Lago Loíza Basin, Puerto Rico showed the percentage of urban and disturbed land as the significant explanatory variables predicting annual sediment concentrations, and the percentage of cropland, pasture, and disturbed land as the three best explanatory variables predicting annual sediment yields (Gellis et al., 2006). In addition to land use, lithology can play a major role in influencing sediment loadings (Godfrey et al., 2008; Larsen and Stallard, 2000; Syvitski and Kettner, 2011). Larsen and Stallard (2000) showed that forested basins in Puerto Rico underlain by intrusive rocks, have sediment yields 3.2 times higher than forested basins underlain by extrusive rocks.

The relation of land use to sediment production in Puerto Rico was demonstrated by Gellis et al. (1999) where sheetwash erosion was measured on 12 slopes under 4 land-use types (cropland, forest, pasture, and urban) from 1991 to 1992 in the Lago Loiza Basin. Erosion reported as an average volume-weighted sediment concentration was highest on construction sites — 61,400 ppm, decreasing on cropland — 45,500 ppm, to pasture — 3430 ppm, and lowest in forest —

2050 ppm. Sediment yields for these land uses ranged from construction sites (0.81 to 9.08 Mg/ha/yr), cropland (0.31 to 0.72 Mg/ha/yr), pasture (0.011 to 0.05 Mg/ha/yr), and forest (0.02 to 0.09 Mg/ha/yr).

1.2. Study basins and sediment availability

Puerto Rico measures 180 km by 65 km and is the smallest island in the Greater Antilles. Puerto Rico is situated on the Caribbean Plate in an oceanic island arc setting that was created in the Early Cretaceous (120 Ma) and active through the Eocene (40 Ma), as the Caribbean Plate was being subducted below Puerto Rico in the Muertos Trough (Donnelly, 1989; Lewis and Draper, 1990). Puerto Rico is volcanic in origin with two main morphotectonic settings: the Central Igneous Zone, composed of volcaniclastic rocks ranging from Late Jurassic to late Eocene and intruded by Late Cretaceous and early Tertiary granitoid rocks, and the Northern and Southern Carbonate Zones, consisting of middle Oligocene through middle Miocene limestones (Monroe, 1980). There are two marked rainfall seasons in Puerto Rico—a drier season, from January through April and a wetter season, from May through December, including the hurricane season. Hurricanes occur on average every 10–20 years (Scatena and Larsen, 1991), and bring intense rainfall, flooding, landslides, and high sediment loading events.

The factors controlling storm-generated suspended-sediment concentrations were investigated in four basins in Puerto Rico: Rio Icacos, Quebrada Blanca, Rio Caguitas, and Rio Piedras, between 1989 and 1995 (Figs. 2 and 3). The 3.26 km^2 Rio Icacos Basin (U.S. Geological Survey (USGS) station ID 50075000) (Figs. 2 and 3a; Table 2) drained a relatively undisturbed forested basin in the Luquillo Experimental Forest (LEF) (Larsen, 1997). Rio Icacos has one of the highest weathering rates in the world (White et al., 1998) and is not sediment-supply limited. It also has high rainfall and runoff and is not transport limited (Shanley et al., 2011). The Rio Icacos has less available sediment because of its forest cover (~100%) and the efficient removal of sediment during most flows. However, during intense storm activity, landslides may occur and become an important sediment source (Larsen and Torres-Sanchez, 1998).

The 8.42 km^2 Quebrada Blanca Basin (USGS station ID 50051150) (Figs. 2 and 3b; Table 2) drains primarily pasture and forest, and is also considered a basin with limited sediment availability. The small amount of cropland (8%) may generate some sediment. The 13.7 km^2 Rio Caguitas Basin (USGS station ID 50055100) (Figs. 2 and 3c and d; Table 2) drains a mixed land use of forest, pasture, cropland, and rural. With almost one-quarter of the basin in cropland (Fig. 3d), Rio Caguitas is a basin with high sediment availability. The 19.4 km^2 Rio Piedras Basin (USGS station ID 50048770) (Figs. 2 and 3e and f; Table 2) drained an urban area within the San Juan metropolitan region. In the 1990s, the San Juan Metropolitan area was experiencing rapid population and housing growth in two districts (barrios) of Rio Piedras, Caimito and Cupey, where population more than tripled between 1960 and 1990 (Gellis, 2003). During the study period (1992–1995), the upper portions of the Rio Piedras Basin that were still forested were undergoing urbanization and large areas of bare ground were present (Gellis, 1991) (Fig. 3f). Gullying and rilling were common on the exposed hillslopes. The Rio Piedras Basin is a basin with a considerable supply of sediment that is available for transport.

Underlying geology can also exert a strong influence on sediment supply. Stallard and Murphy (2012) and Larsen (2012) showed that basins in Puerto Rico underlain by granitic rocks have higher sediment yields than basins underlain by volcaniclastics. However it was also shown that anthropogenically disturbed basins in Puerto Rico still showed the highest sediment yields (Larsen, 2012). The four study basins have both rock types (Table 2), with Rio Icacos and Quebrada Blanca draining dominantly quartz diorite and granodiorite, respectively and Rio Caguitas and Rio Piedras draining
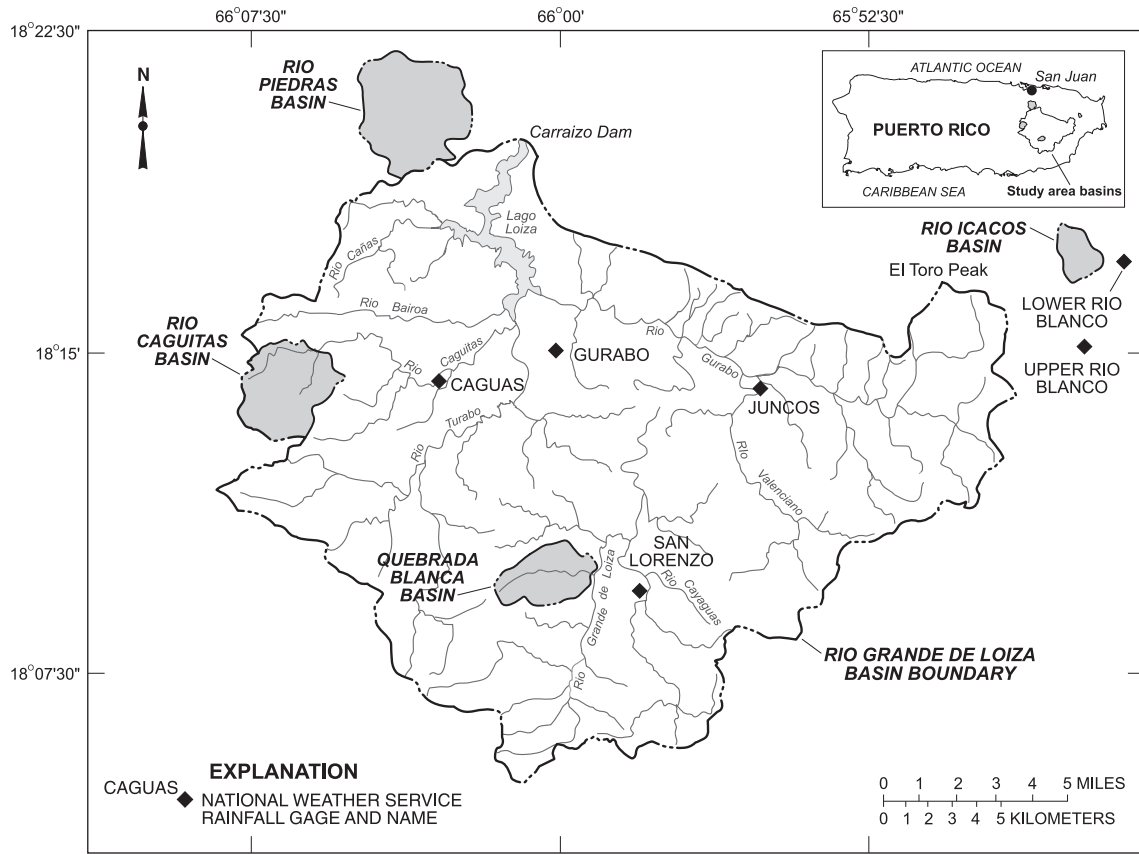
Fig. 2. Location of four study basins: Rio Icacos, Quebrada Blanca, Rio Caguitas, and Rio Piedras.
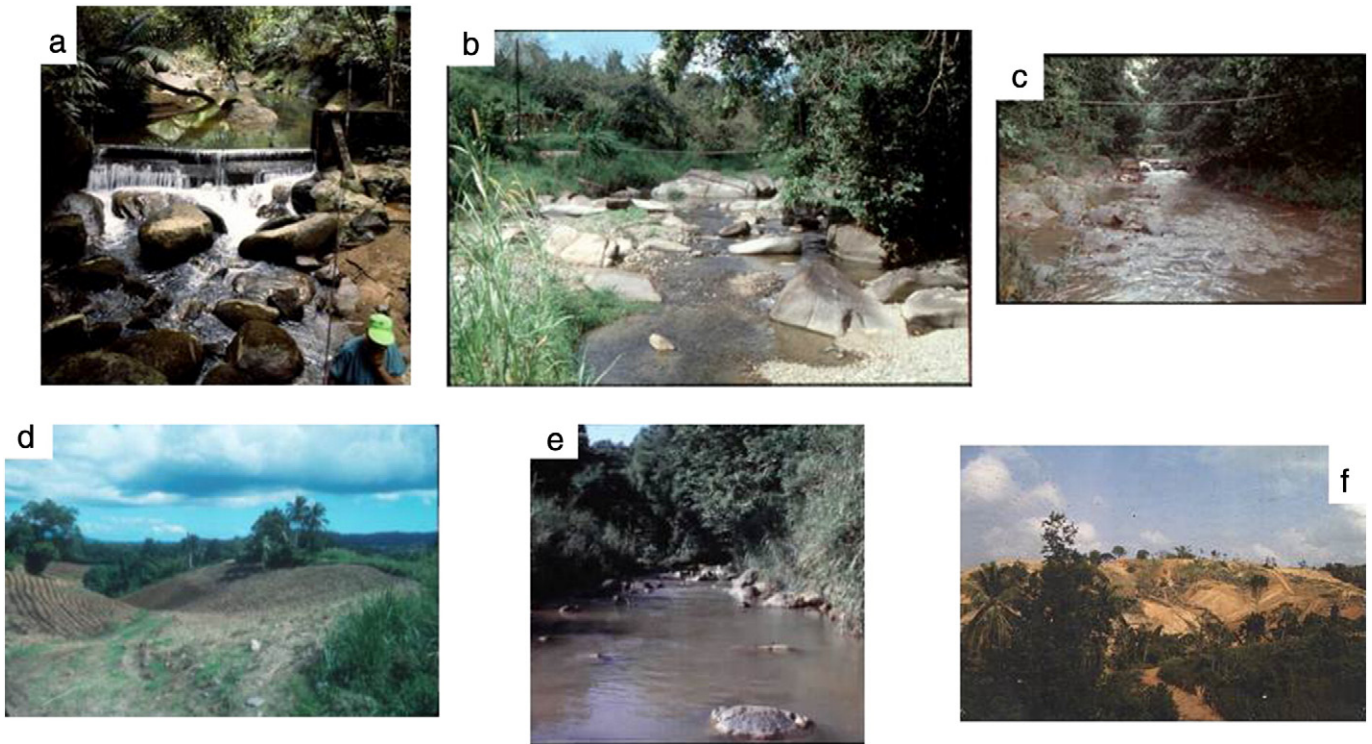

Fig. 3. Photographs of the four study basins. a) view looking upstream of Rio Icacos near the USGS streamflow station (1984), b) view looking upstream of Quebrada Blanca near the USGS streamflow station (1989), c) view looking downstream of Rio Caguitas near the USGS streamflow station Rio Caguitas near Aguas Buenas (1992), d) cropland in the Rio Caguitas Basin (1995), e) view looking upstream of Rio Piedras near the USGS streamflow station Rio Piedras near Senorial (1999), and f) urbanization in the Rio Piedras Basin (1995).

Table 2
Physical and land use attributes of study watersheds.

Basin	Drainage area, km²	Geology	Soils	Land use (%)	Elevation range, m amsl	Average annual precipitation, mm	Watershed slope, %	Mean channel slope near gaging station, %	D50 channel bed, mm[h]
Rio Icacos	3.26	Quartz diorite[a]	Utuado loam[e]	Forest (~100)[b]	616 to 752	2500 to 5000	22.2[b]	7.3[b]	0.6
Quebrada Blanca	8.42	Granodiorite and volcaniclastic rocks[a]	Pandura sandy loam, Mucara clay[f]	Pasture (54) Forest (21) Rural (15) Cropland (8)[c]	140 to 642	1831	33.4[h]	3.4[h]	19
Rio Caguitas	13.7	Volcaniclastic rocks[a]	Mucara clay[f]	Pasture (27) Forest (36) Rural (11) Cropland (23)	120 to 450	1648	33.2[h]	7.1[h]	8
Rio Piedras	19.4	Volcaniclastic rocks and quartz diorite[d]	Humatas clay[f]	Urban (77) Forest (23)[h]	30 to 300	1951	17.6[g]	1.2[i]	2

[a] Briggs and Akers (1965).
[b] Larsen (1997).
[c] Gellis et al. (1999).
[d] Pease (1968).
[e] Boccheciamp (1977).
[f] Boccheciamp (1978).
[g] Based on GIS analysis from 10×10 m DEM.
[h] Gellis (2003).
[i] Slope near streamflow station was determined from USGS Aguas Buenas 1:20,000 topographic map.

dominantly volcaniclastics (Briggs and Akers, 1965; Lugo et al., 2011; Pease, 1968).

2. Data assemblage and statistical methods

A statistical model of storm-generated sediment transport in the four study basins was developed through analysis of storm-generated sediment loads and concentrations. Important meteorologic and hydrologic variables in sediment transport were characterized for five 5 flow periods: (1) the current storm hydrograph, (2) the flow and rainfall since the previous storm event, (3) the previous storm event, (3) 2nd previous storm event, and (4) the 3rd previous storm storm event.

2.1. Meteorologic, hydrologic, and sedimentologic data

Rainfall used in this analysis was recorded at the USGS streamflow-gaging station in each of the four study basins, in selected areas in the study basins, and in neighboring basins. Rainfall recorders were tipping-bucket type raingages that were programmed to report rainfall totals every 15 min. Rainfall for a storm event was determined using a Thiessen weighted average.

Streamflow measurements were made monthly on a routine basis and during high flows. Streamflow was measured and computed at each station following USGS protocols (Kennedy, 1984). Using the relation of stage and discharge, discharge was computed on 15-minute intervals. Suspended-sediment samples were collected during a range of flows at each station. Low- and high-flow suspended-sediment samples were collected using conventional USGS depth-integrating isokinetic samplers using the equal-width-increment (EWI) method (Edwards and Glysson, 1988). All of the streamflow-gaging stations were fitted with an automatic pump sampler that was activated during high river stage and collected up to 24 separate, sequential water-sediment samples. The activation stage was typically between base flow and bankfull flow. The time intervals between samples were based on previous analysis of hydrographs for each stream to sample the entire flood hydrograph. The automatic samplers collected sediment from a point in the channel. To account for any bias in sampling at a point, at selected times an EWI was taken with isokinetic samplers and compared to the automatic samples. If necessary, a correction coefficient was applied to the samples collected from the automatic sampler (Edwards and Glysson, 1988). Suspended-sediment samples were analyzed for concentration at the USGS Caribbean District sediment laboratory in Puerto Rico. Determination of suspended-sediment concentration was made by the evaporation or filtration method (Guy, 1969).

To assemble the best dataset for statistical analysis, only suspended-sediment data from events where samples covered the entire storm hydrograph (rising and falling limbs) were selected. The suspended-sediment load for an event was computed by developing a continual trace of suspended-sediment concentration over the hydrograph and subdividing by time (Porterfield, 1972).

For short time periods between samples (hours) when suspended sediment was not sampled, two methods were used to estimate suspended-sediment concentration. If the time of the estimated suspended-sediment concentration was reasonably close in time to other samples (<120 min) and the flow stage (rising or falling) was unchanging between samples, a linear interpolation was used to estimate the suspended-sediment concentration. For other time gaps, sediment-transport curves for the specific event were made by plotting rising and falling limb instantaneous discharge and suspended-sediment concentration. Lines of best fit that were generated for the rising and falling limb portions of the transport curves were used to estimate suspended-sediment concentration. The type of hysteresis for each storm was defined visually based on Fig. 1.

2.2. Definition of a runoff event

Rules were established to define a runoff event and peakflow in an event. In each of the four study basins, a runoff event was defined by a minimum peakflow. Hourly discharges for the period of study for each station were ranked to obtain the 95th percentile of discharge. The flow selected from the 95th percentile analysis was as the minimum peakflow that defined an event. The minimum peak discharges used to define an event for each of the study basins are shown in Table 3.

The start of runoff events was easy to discern for most events in the four basins as an abrupt rise in discharge. It was more difficult to determine when the runoff events ended. For consistency, a methodology was developed to define the end of the runoff event (Fig. 4a). The end of the runoff event was based on graphical features of the recessional portion of the hydrograph where a break in the maximum curvature of the recession curve or inflection point was selected as the point where surface flow ceases and base flow begins. The inflection point on the hydrograph recession curve was obtained by taking the second derivative of a 3rd-order best-fit regression line to the

Table 3
Hydrologic parameters used to define an event, the end of an event, a complex event, and the end of a complex event.

Study basin	Minimum peak discharge used to define an event(m^3/s)	Minimum peak discharge per unit basin area (m^3/s/km^2)	Threshold base flow used to define the end of an event (m^3/s)	Threshold recession limb slope over minimum listed hours used to define the end of an event	Threshold discharge used to define complex event (m^3/s)	Threshold recession limb slope used to define end of complex event (m^3/s/h) over listed hours
Rio Icacos	0.85	0.261	0.28	0.0005 m^3/s over 2.0 h	0.48	0.014 m^3/s over 2 h
Quebrada Blanca	0.42	0.050	0.34	0.0001 m^3/s over 2.5 h	0.42	0.014 m^3/s over 2 h
Rio Caguitas	0.34	0.025	0.34	0.0003 m^3/s over 2.5 h	0.45	0.014 m^3/s over 2 h
Rio Piedras	1.36	0.070	0.28	0.0002 m^3/s over 2.0 h	0.57	0.014 m^3/s over 2 h

recession portion of the hydrograph (Fig. 4a). The second derivative of a 3rd-order equation is the inflection point of the curve or where concavity changes (Hughes-Hallett, 1994). In order for the inflection point to be considered the end of the event, the recessional limb of the storm hydrograph had to fall below a threshold base flow and reach a threshold slope (Table 3). The threshold base flow and slope of the recessional limb of the storm hydrograph were based on analysis of base-flow recession curves.

Events that are closely spaced in time are designated as "complex events" (Fig. 4b). In complex events, the recessional portions of the storm hydrographs approach but never reach base flow as defined for regular events. However, the individual runoff portions that make up the complex event may be considered isolated because discrete rainfall events are responsible for each rise in runoff. If a portion of a complex event was not sampled, it was ignored.
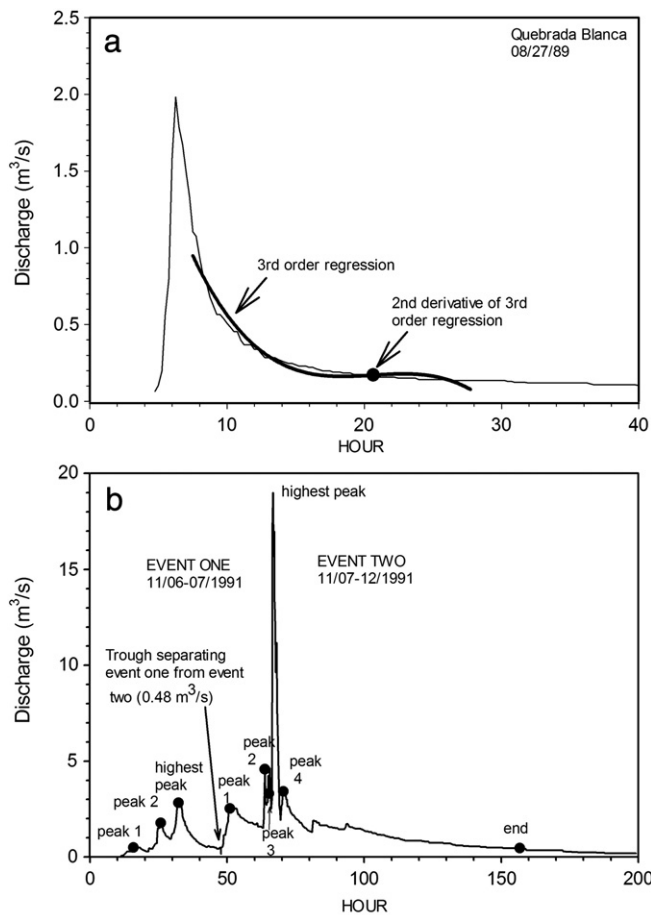
Fig. 4. a. Example of how the end of the event was determined by taking the 2nd derivative of a 3rd order regression fit to the falling limb of the hydrograph. The hydrograph used is from Quebrada Blanca for an event that occurred on 8/27/1989. b. Example of a complex runoff event with several peakflows at Quebrada Blanca near El Jagual (11/6/1991 to 11/12/1991).

Complex event hydrographs were delineated into separate runoff events based on the following criteria. A threshold discharge and a threshold slope were developed for the recessional portion of the hydrograph for each basin (Table 3). The threshold discharge was based on examination of recession curves and was always higher than the value used to determine the end of a single event (Table 3). If the hydrograph recession met the threshold discharge and threshold slope criteria, the end of that portion of the complex event was selected just before the next hydrograph rise. The final recession limb of the complex event had to meet the criteria established for a single event.

The number of peaks in an event and their magnitudes are variables that can influence suspended-sediment characteristics (Walling, 1974). Some runoff events only have one peak, and the peak-flow characteristics are only defined for that peak. Other events are multi-peaked, defined by troughs and peaks. For multi-peaked events, a peak is defined by a minimum difference in discharge from the immediately preceding trough to the peak (Table 4). The minimum difference in discharge used to define each peak varied over a range of discharges. At each streamflow-gaging station, an analysis was made of peakflow minus the preceding trough flow. The peakflows were categorized into classes of 0–2.83 m^3/s, 2.83–14.2 m^3/s, and >14.2 m^3/s. The minimum value obtained by subtracting the preceding trough flow from the peakflow in each class was used to define a minimum peakflow in a multi-peaked event (Table 4). Although some of the rules used to define hydrologic characteristics in Tables 3 and 4, such as the designation of the peakflow classes, may be considered qualitative, they nevertheless provided standardization in the statistical analysis among different watersheds.

2.3. Statistical analysis of storm-generated sediment loads and concentrations

Two response variables were used to describe sediment for the entire runoff event: (1) suspended-sediment load) and (2) the discharge-weighted sediment concentration. Discharge-weighted sediment concentration (mg/L) is a variable computed as suspended-sediment load (Mg) divided by the total runoff of the event (m^3).

The explanatory variables tested as significant in controlling suspended-sediment load and the discharge-weighted sediment concentration consisted of meteorological and hydrologic data that were

Table 4
Difference in the peakflow minus the preceding trough used to define a peak in a multi-peaked event. [NA = not applicable].

Discharge of trough preceding peakflow in multi-peaked event (m^3/s)	Difference in discharge (peakflow minus trough) (m^3/s)			
	Rio Icacos	Quebrada Blanca	Rio Caguitas	Rio Piedras
>0 to 2.83	0.28	0.28	0.28	0.57
>2.83 to 14.16	1.27	1.42	1.13	1.42
>14.16 to 28.32	NA	NA	4.25	2.83

categorized into five flow periods (Table 5). Skoklevski and Velickov (1995) observed that the best correlations of sediment for rivers in the Republic of Macedonia were observed for rising runoff and falling limb runoff. Loughran (1977) and Sharma et al. (1992) categorized suspended-sediment samples relative to peak discharge, into samples on the rising and falling limbs. To test whether sediment loads (SED, SEDPK, and SEDAFTPK) and sediment concentrations (CONC, CONCPK, and CONCAFTPK) showed differing explanatory variables for different portions of the storm hydrograph, three portions of the storm hydrograph were analyzed: (1) the entire storm hydrograph, (2) to the highest peakflow, and (3) after the highest peakflow (Table 5). To account for varying time periods since the previous storm event(s), runoff and precipitation since the previous storm event(s) were divided by the time from the end of the previous storm event to the beginning of the current event. In complex events, the time since the previous event for the second and higher peaks on the hydrograph was 15 min which is the time between reported discharge values. Normalizing by

time assumes that recent storms have a greater effect on sediment than events further back in time.

In addition to statistical analysis on loads and concentrations, analysis was also performed on the variables controlling hysteresis (sediment exhaustion and sediment increases) for the entire storm hydrograph (Table 5). Only sediment samples that were collected were used in the statistical analysis of hysteresis; estimated suspended-sediment concentrations were not used. With hysteresis being defined by use of concentration results from samples collected at similar discharges on the rising and falling limbs, only samples that were collected at similar discharges on the rising and falling limbs were used. In the analysis of hysteresis for the four study basins, the lowest discharge values examined on the rising and falling limbs ranged from 0.1 to 36% of each other and the highest discharge values examined on the rising and falling limbs ranged from 0 to 25% of each other.

The response variable used to describe hysteresis (CONC_DIFF) is computed as the difference of the average sediment concentration

Table 5
Response and explanatory variables used in the statistical analysis of suspended-sediment loads and concentrations.

Response variables

Abbreviation used in text	Explanation
SED[a]	Sediment load for the entire event, Mg
SEDPK[b]	Sediment load to the highest peakflow, Mg
SEDAFTPK[c]	Sediment load after the highest peakflow, Mg
CONC[a]	Discharge-weighted sediment concentration for the entire event, mg/L
CONCPK[b]	Discharge-weighted sediment concentration to the highest peakflow, mg/L
CONCAFTPK[c]	Discharge-weighted sediment concentration after the highest peakflow, mg/L
CONC_DIFF[d]	Difference of average sediment concentration (mg/L) on the rising limb minus the average sediment concentration on the falling limb (mg/L)

Explanatory variables

Abbreviation used in text	Explanation	Abbreviation used in text	Explanation
1-RUN[a]	Runoff, m³	16-RULST[a,b,c,d]	Previous storm event runoff divided by the time since the previous storm event, m³/s/h
1A-RUNTOPK[b]	Runoff to the highest peakflow, m³	17-PPTLSTI[a,b,c,d]	Previous storm event rainfall divided by the time since previous storm event, mm/h
1B-RUNAFTPK	Runoff after the highest peakflow, m³	18-INTLST[a,b,c,d]	Previous storm event maximum 15-minute rainfall intensity divided by the time since the previous storm event, mm/h
2-BASE[a,b,d]	Base flow at start of the event, m³/s	19-75LST[a,b,c,d]	Previous storm event 75% rainfall intensity divided by the time since the previous storm event, mm/h
3-PK[a,b,c,d]	Peakflow, m³/s	20-LSPKTI2[a,b,c,d]	2nd previous storm event maximum peakflow divided by the time since the 2nd previous storm event, m³/s/h
4-MXTMJPK[a,b]	Maximum rate of hydrograph rise to the highest peakflow, m³/s	21-SMLSPK2[a,b,c,d]	2nd previous storm event sum of peakflows divided by the time since the 2nd previous storm event, m³/s/h
5-MXTRPK[a,d]	Maximum rate of hydrograph rise to any peakflow, (m³/s)/min	22-RULST2[a,b,c,d]	2nd previous storm event runoff divided by the time since the 2nd previous storm event, m³/s/h
6-SMPK[a,d]	Sum of peakflows, (m³/s)/min	23-PPTLSTI2[a,b,c,d]	2nd previous storm event rainfall divided by the time since the 2nd previous storm event, mm/h
7-TOTRAIN[a,d]	Total rainfall for event, mm	24-INTLST2[a,b,c,d]	2nd previous storm event maximum 15-minute rainfall intensity divided by the time since the 2nd previous storm event, mm/h
8-INT15[a,d]	Maximum 15-minute rainfall intensity, mm/15 min	25-75LST2[a,b,c,d]	2nd previous storm event 75% total rainfall divided by the time since the 2nd previous storm event, mm/h
9-INT75[a,d]	75% of total rainfall for the event divided by time in which it fell, mm/h	26-LSPKTI3[a,b,c,d]	3rd previous storm event maximum peakflow divided by the time since the 3rd previous storm event, m³/s/h
10-RRISE[a,b,d]	Rainfall totals to highest peakflow, mm	27-SMLSPK3[a,b,c,d]	3rd previous storm event sum of peakflows divided by the time since the3rd previous storm event, m³/s/h
11-RAINFOL[a,c,d]	Rainfall totals after highest peakflow, mm	28-RULST3[a,b]	3rd previous storm event runoff divided by the time since the 3rd previous storm event, m³/s/h
12-RNBTWTI[a,b,c,d]	Runoff occurring since previous storm event, m³/h	29-PPTLSTI3[a,b]	3rd previous storm event rainfall divided by the time since the 3rd previous storm event, mm/h
13-PPTBTW[a,b,c,d]	Rainfall occurring since previous storm event divided by the time since the previous storm event, mm/h	30-INTLST3[a,b,c,d]	3rd previous storm event maximum 15-minute rainfall intensity divided by the time since the 3rd previous storm event, mm/h
14-LSPKTI[a,b,c,d]	Previous storm event maximum peakflow divided by the time since the previous storm event, m³/s/h	31-75LST3[a,b,c,d]	3rd previous storm event 75% total rainfall divided by the time since the 3rd previous storm event, mm/h
15-SMLSPK[a,b,c,d]	Sum of previous storm event peakflows divided by the time since the previous storm event, m³/s/h		

[a] Used in the statistical analysis for the entire event.
[b] Used in the statistical analysis to the highest peakflow.
[c] Used in the statistical analysis after the highest peakflow.
[d] Used in the statistical analysis for hysteresis.

on the rising limb minus the average sediment concentration on the falling limb. A weighted average of sediment concentration was calculated for the rising and falling samples, as follows:

$$CONC_{DIFF} = SCr - SCf \qquad (1)$$

$$SCr \text{ or } SCf = \sum_{i=1}^{i=n} Conc(i) \cdot \frac{t_i}{t_T} \qquad (2)$$

where SCr is the average sediment concentration (mg/L) for the rising limb portion of the hydrograph to the highest peakflow; SCf is the average sediment concentration (mg/L) for the falling limb portion of the hydrograph after the highest peakflow; n = total number of the samples (i) collected on either the rising or falling limb; Conc(i) = suspended-sediment concentration of sample i; t_i = hours representative of sample i, determined as half the time period to the previous sample plus half the time period to the next sample; t_T = total time (h) of sample collection on either the falling or rising limb.

A higher value of hysteresis would indicate that sediment exhaustion occurred over the hydrograph leading to storms with TYPE-1 hysteresis. A lower value of hysteresis would indicate that less sediment is transported on the rising limb relative to the falling limb, leading to TYPE-3 hysteresis. Williams (1989) used a similar approach to determine the increase or decrease in suspended sediment for an event by taking the ratio of suspended-sediment concentration to discharge (C/Q) at the same discharge, for the widest parts of the hysteresis loop. Explanatory variables used to determine which factors influence hysteresis during an event were similar to the analysis for the entire event (Table 5).

2.4. Statistical procedures

Factor analysis using Principal Components Analysis (PCA) to extract the factors was performed on the ranked data, and stepwise regression was performed on the factor scores. All statistical tests were run using the SAS software package (Statistical Analysis System, 1989[1]). The SAS PROC FACTOR command was used in factor analysis and PROC REG was used in stepwise regression.

Factor analysis using PCA was used to reduce the dimensionality of the data scatter onto a new set of axes and compute new composite variables that are uncorrelated (Davis, 1986). Factor scores represent the original data projected onto the new axes. In factor analysis, a smaller number of factors are selected to determine a simplified structure to the data (Davis, 1986). In this statistical analysis, the number of components or factors selected was based on the number needed to account for a cumulative percent of variance of at least 85% (Cattell, 1966; Kaiser, 1960). Rotation of the factor axes can be used to simplify the loading structure, and achieve a more meaningful and interpretable solution (Daultrey, 1976; Davis, 1986). Rotation of the factors was performed using the varimax rotation. Stepwise regression was then performed using the factor scores after rotation as explanatory variables against the response variables of suspended-sediment load and discharge-weighted sediment concentration for all three portions of the hydrograph, and hysteresis, with the probability level of significance set at 0.05 for all tests.

Regression analysis of factor scores is a common way to examine data, although there is disparity in the literature with respect to treatment of the data prior to the multivariate analysis (Baxter, 1995; Reid and Spencer, 2009). In a study of factors influencing sediment geochemical data from an estuary in SE England, Reid and Spencer (2009) showed that log transformations of the data masked important trends, while removing outliers had the most significant effect on PCA outputs

and data interpretation. Baxter (1995) compared PCA analysis using raw data, logarithmically transformed data, and ranked data and found that no single approach could be recommended, but suggested that ranked data were more robust to outliers and may indicate structure to the data not shown by the other methods. Heywood et al. (1980) performed PCA on ranked data to classify eutrophication in lakes of the South Orkney Islands.

As part of this analysis to determine whether the data should be treated prior to analysis, factor analysis was performed on the raw data, normalized data, and ranked data for all four basins. Factor analysis on the raw and normalized data used the correlation matrix as input. Results indicated that all approaches provided similar results with the ranked data showing the highest R^2 and lowest probability values. Ranking the data may prevent issues associated with variables having different units. Ranked data were subsequently used in this analysis by assigning the lowest value a rank of 1.

3. Results

3.1. Rio Icacos — sediment data

Suspended sediment that was collected at Rio Icacos near Naguabo from May 5, 1992 through September 20, 1994 was used in the statistical analysis. For this period, the mean daily flow was 0.29 m³/s. For the longer period of record, July 1, 1945 through September 30, 2006, the mean daily flow was 0.39 m³/s; indicating that the period of study occurred during a drier than average flow period.

From May 5, 1992 through September 20, 1994, 630 water samples were collected for suspended-sediment concentration at Rio Icacos near Naguabo. Of these samples, 72 were collected during base flow, 240 on the rising limb of the hydrograph to the highest peak, and 318 on the recessional limb of the hydrograph. Boxplots of the data show that the 10th, 25th, 50th, 75th, and 90th percentiles of suspended-sediment concentration are 20; 110; 241; 467; and 850 mg/L, respectively (Fig. 5a). Rio Icacos had the lowest suspended-sediment concentration to discharge per unit area for any of the four basins (Fig. 5b). Although weathering rates are high in the Rio Icacos (White et al., 1998), the Icacos has less available sediment because of its forest cover and the efficient removal of sediment during most flows.

For the period May 5, 1992 through September 20, 1994, 194 runoff events, defined by a peakflow over 0.85 m³/s, occurred. Of these runoff events, 48 were sampled adequately to define suspended-sediment load for the entire event (Supplemental Table A.1). Peakflows for the current and past events, with the exception of three events (5/23/1992, 2/19/1994, and 2/19–20/1994) can be characterized as small events with recurrence intervals of less than 1.25 years (Supplemental Table A.1).

3.2. Rio Icacos — statistical results

Results of stepwise regression on the factor scores for Rio Icacos show that factors with high loadings on rainfall, peakflow, and runoff of the current event are significant and positively correlated with the response variables of sediment load and sediment concentration for all three portions of the hydrograph (Table 6). Factors with high loadings on previous event rainfall, peakflow, and runoff are significant in the third step of stepwise regression and are positively correlated to sediment loads (Table 6). Factors with high loadings on the 3rd previous event are positively correlated to sediment load (SEDPK) and sediment concentration to the highest peakflow (CONCPK) (Table 6). Runoff and rainfall of the current storm event and 3rd previous storm event are supplying sediment to the rising limb of the hydrograph (Table 6). Factors with high loadings on the runoff since the previous storm event (12-RNBTWTI) are negatively correlated to sediment load and sediment concentration to the highest peakflow, indicating that runoff since the previous storm event was flushing sediment that would have been
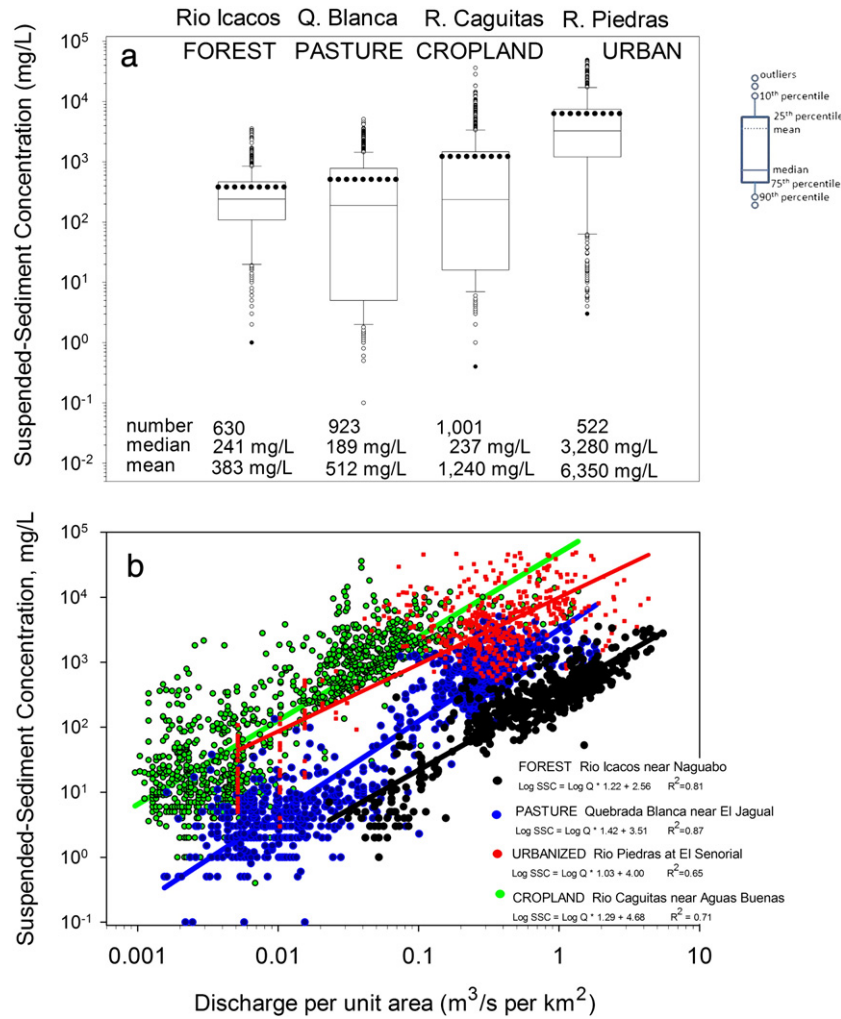

Fig. 5. a. Boxplots of suspended-sediment concentrations for the four study basins. b. Suspended-sediment concentrations versus discharge per unit area for the four study basins.
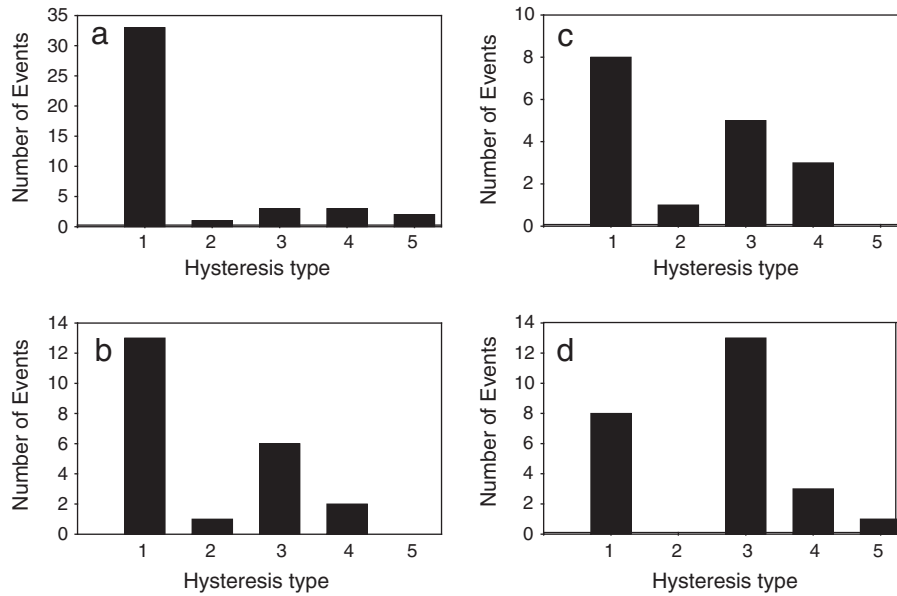
made available to the rising limb of the hydrograph (Table 6). Loadings on base flow (2-BASE) at the start of the event are significant in the fourth step of stepwise regression and are positively correlated with current event sediment load (Table 6). Higher base flow at the start of

the runoff event may reflect wetter soil moisture conditions in the basin leading to higher runoff and higher sediment loads.

Hysteresis loops were examined for the 42 sampled events. Hysteresis TYPE-1 (clockwise) is most common (Fig. 6a), occurring in

Table 6
Results of stepwise regression on factor scores for different portions of the hydrograph, Rio Icacos.

Portion of hydrograph	Response variable	Number of factors used in regression and variance explained	Significant factors	R^2	P value	Factor loadings and correlation of explanatory to response variables. A '+' indicates a positive correlation of the explanatory variable(s) to the response variable; a '−' indicates a negative correlation of the explanatory variable(s) to the response variable. See Table 5 for list of abbreviations.
Entire	SED	7:87%	Step 1: FACTOR3	0.68	0.0001	>0.8(1-RUN, 6-SMPK,7-TOTRAIN,10-RRISE,11-RFALL)+
			Step 2: FACTOR5	0.88	0.0001	>0.8(4-MXTMJPK,5-MXTRPK)+
			Step 3: FACTOR1	0.90	0.0032	>0.8(14-LSPKTI, 15-SMLSPKTI, 16-RULST, 17-LSTPPTI, 18-INTLST, 19-75LST)+, <-0.5(13-PPTBTW)−
			Step 4: FACTOR7	0.91	0.0369	>0.8(2-BASE)+
Entire	CONC	7:87%	Step 1: FACTOR5	0.44	0.0001	>0.8(4-MXTMJPK, 5-MXTRPK)+
			Step 2: FACTOR3	0.72	0.0001	>0.7(6-SMPK, 7-TOTRAIN, 8-INT15, 10-RRISE, 11-RFALL)+
To the highest peak	SEDPK	6:87%	Step 1: FACTOR4	0.41	0.0001	>0.7(1A-RUNTOPK, 3-PK, 10-RRISE)+
			Step 2: FACTOR5	0.66	0.0001	<-0.6(4-MXTMJPK)+, >0.7(12-RNBTWTI)−
			Step 3: FACTOR2	0.70	0.0126	>0.8(26-LSPKTI3,27-SMLSPK3,28-RULST3,29-PPTLSTI3,31-INTLST3)+
To the highest peak	CONCPK	6:89%	Step 1: FACTOR5	0.65	0.0001	>0.7(3-PK, 4-MXTMJPK,10-RRISE)+
			Step 2: FACTOR2	0.70	0.0145	>0.8(26-LSPKTI3, 27-SMLSPK3, 28-RULST3, 29-PPTLSTI3, 30-INTLST3)+
			Step 3: FACTOR5	0.74	0.0138	>0.8(12-RNBTWTI)−
After the highest peak	SEDAFTPK	6:89%	Step 1: FACTOR3	0.48	0.0001	>0.8(3-PK, 4-MXTMJPK)+
			Step 2: FACTOR5	0.85	0.0001	>0.7(1B-RUNAFTPK, 11-RAINFOL)+
After the highest peak	CONCAFTPK	6:89%	Step 1: FACTOR4	0.61	0.0001	>0.8(3-PK, 4-MXTMJPK)+
Hysteresis	CONC_DIFF	7:87%	Step 1: FACTOR4	0.13	0.02	>0.7(3-PK, 8-INT-15, 10-RRISE, 11-RFALL)+

Fig. 6. Frequency of hysteresis loops in each basin for (a) Rio Icacos near Naguabo for the entire event, (b) Quebrada Blanca near El Jagual, (c) Rio Caguitas near Aguas Buenas, and (d) Rio Piedras near El Senorial (see Fig. 1 for definition of loop types).

33 events, TYPE-2 in 1 event, TYPE-3 in 3 events, TYPE-4 in 3 events, and TYPE-5 in 2 events (Fig. 6a; Supplemental Table A.1).

Stepwise regression on the factor scores versus hysteresis (CONC_DIFF) shows that FACTOR4 with high loadings on the rainfall and peakflow of the current event is significant in explaining sediment exhaustion during the storm hydrograph (Table 6). High, fast rising peakflows, which are a function of rainfall intensity and runoff, led to greater sediment exhaustion through the storm hydrograph.

3.3. Quebrada Blanca — sediment data

Suspended sediment that was collected at Quebrada Blanca near El Jagual from March 8, 1989 through September 30, 1993 was used in the statistical analysis. For this period, the mean daily flow was 0.15 m^3/s. For the longer period of record, October 1, 1984 to September 30, 2002, the mean daily flow was 0.19 m^3/s; therefore, the period of study occurred during a drier than average flow period.

From March 8, 1989 through September 30, 1993, 923 water samples were collected for suspended-sediment concentration at Quebrada Blanca near El Jagual. Of these samples, 374 were collected during base flow, 212 were collected on the rising limb of the hydrograph to the highest peak, and 337 on the recessional limb of the hydrograph. Boxplots of the data show that the 10th, 25th, 50th, 75th, and 90th percentiles of suspended-sediment concentration are 2.0; 5.0; 189; 786; and 1440 mg/L, respectively (Fig. 5a). Quebrada Blanca showed the 2nd lowest suspended-sediment concentration to discharge per unit area for any of the four basins (Fig. 5b).

For the period March 8, 1989 through September 30, 1993, 153 run-off events defined by a peakflow over 0.42 m^3/s occurred. Of these runoff events, 23 were sampled adequately to define suspended-sediment load for the entire event (Supplemental Table A.2). Peakflows for the current and past events, with the exception of two events (5/16–17/1992 and 7/22–23/1993) had recurrence intervals of less than 1.25 years (Supplemental Table A.2).

3.4. Quebrada Blanca — statistical results

Results of stepwise regression on the factor scores show that factors with high loadings on rainfall, peakflow, and runoff are positively correlated with the response variables of sediment load and sediment concentration for all three portions of the hydrograph (Table 7). Using sediment load to the highest peakflow (SEDPK) as the response

Table 7
Results of forward stepwise regression on principal components for different portions of the hydrograph, Quebrada Blanca.

Portion of hydrograph	Response variable	Number of factors used in regression and variance	Significant factors	R^2	P value	Factor loadings and correlation of explanatory to response variables. A '+' indicates a positive correlation of the explanatory variable(s) to the response variable; a '−' indicates a negative correlation of the explanatory variable(s) to the response variable. See Table 5 for list of abbreviations.
Entire	SED	7:90%	Step 1: Factor4	0.53	0.0001	>0.7(1-RUN, 6-SMPK, 7-TOTRAIN, 11-RAINFOL)+
			Step 2: Factor5	0.68	0.0078	>0.8(4-MXTMJPK, 5-MXTRPK)+
Entire	CONC	7:90%	Step 1: Factor5	0.45	0.0005	>0.7(4-MXTMJPK, 5-MXTRPK)+
			Step 2: Factor4	0.57	0.0264	>0.7(6- SMPK, 7-TOTRAIN, 11-RAINFOL)+
To the highest peak	SEDPK	6:89%	Step 1: Factor6	0.59	0.0001	>0.8(1A-RUNTOPK) +
			Step 2: Factor5	0.71	0.0106	<0.8(4-MXTMJPK) +
			Step 3: Factor3	0.77	0.0396	>0.8(14-LSPKTI, 15-SMLSPK, 16-RULST)+
To the highest peak	CONCPK	6:90%	Step 1: Factor4	0.44	0.0006	>0.9(4-MXTMJPK)+
After the highest peak	SEDAFTPK	6:89%	Step 1: Factor4	0.41	0.0009	>0.7(1B-RUNAFTPK, 11-RAINFOL)+
			Step 2: Factor6	0.61	0.0054	>0.6(3-PK, 4-MXTMJPK)+
After the highest peak	CONCAFTPK	6:89%	Step 1: Factor5	0.43	0.0007	>0.9(3-PK, 4-MXTJPK)+
Hysteresis	CONC_DIFF	7:92%	Step 1: Factor6	0.18	0.09*	>0.8(11-RAINFOL) −

* A variable was not found significant until the p-value equaled 0.09.

variable shows that FACTOR3 with high loadings on the previous storm peakflow and runoff are significant in the third step of stepwise regression, and are positively correlated, indicating that runoff and peakflow of the previous storm event are supplying sediment to the rising limb portion of the current event (Table 7).

Hysteresis loops were examined for 22 events (Supplemental Table A.2). Hysteresis TYPE-1 (clockwise) is most common (Fig. 6b), occurring in 13 events, TYPE-2 in 1 event, TYPE-3 in 6 events, and TYPE-4 in 2 events (Fig. 6b).

Stepwise regression on the factor scores versus hysteresis (CONC_DIFF) shows that FACTOR6, with high loadings on rainfall on the falling limb (11-RAINFOL) is significant in explaining sediment exhaustion during the storm hydrograph (Table 7). Rainfall on the falling limb is negatively correlated to hysteresis, indicating that higher rainfall on the falling limb increased sediment and led to less sediment exhaustion during the storm hydrograph.

3.5. Rio Caguitas — sediment data

Suspended sediment that was collected at Rio Caguitas near Aguas Buenas from November 25, 1991 through May 23, 1996 was used in the statistical analysis. For this period, the mean daily flow at Rio Caguitas near Aguas Buenas was 0.18 m³/s. For the longer period of record, February 13, 1990 through September 20, 2003, the mean daily flow was 0.22 m³/s; therefore, the period of study occurred during a drier than average flow period.

From November 25, 1991 through May 23, 1996, 1001 water samples were collected for suspended-sediment concentration at Rio Caguitas near Aguas Buenas. Of these samples 515 were collected during base flow, 127 were collected on the rising limb of the hydrograph to the highest peakflow, and 359 were collected on the recessional limb of the hydrograph. Boxplots of the data show that the 10th, 25th, 50th, 75th, and 90th percentiles of suspended sediment are 7.0; 16; 237; 1470; and 3350 mg/L, respectively (Fig. 5a). Rio Caguitas had the highest suspended-sediment concentration to discharge per unit area for any of the four basins (Fig. 5b).

For WYs 1991 through 1996, average suspended-sediment load, sediment yield, and discharge-weighted sediment concentrations were 8290 Mg, 602 Mg/km²/yr, and 1360 mg/L, respectively. For WYs 1991 through 1996, 90% of the average suspended-sediment load was transported in 12 days, 75% in 5 days, and 47% in 1 day.

For the period November 25, 1991 through May 23, 1996, 127 runoff events defined by a peakflow over 0.34 m³/s occurred. Of these runoff events, 23 were sampled adequately to define suspended-sediment load for the entire event (Supplemental Table A.3). Peakflows for the current and past events, with the exception of 6 events (1/5/1992, 12/29/1992, 1/7/1993, 5/26/1993, 9/6/1995, and 9/15/1995) had recurrence intervals of less than 1.25 years (Supplemental Table A.3).

3.6. Rio Caguitas — statistical results

Results of stepwise regression on the factor scores show that factors with high loadings on rainfall, peakflow, and runoff of the current event are significant and are positively correlated with the response variables of sediment load and sediment concentration for all three portions of the hydrograph (Table 8). Rainfall since the previous event (13-PPTBTW) is positively correlated to sediment concentration for the entire event (CONC) and to the concentration after the highest peakflow (CONCAFTPK) (Table 8). Sediment load after the highest peakflow (SEDAFTPK) is negatively correlated to runoff since the previous storm event (12-RNBTWTI). Factors with high loadings on rainfall of the 2nd previous storm event are negatively correlated with the sediment load and concentration for the entire event and to the highest peakflow, and factors with high loadings on the 3rd previous event are negatively correlated to concentration to the highest peakflow (CONCPK) (Table 8). Sediment concentration to the highest peakflow (CONCPK) is negatively correlated with peakflow, runoff, and rainfall of the 3rd previous event (Table 8).

Hysteresis loops were examined for 17 sampled events. Hysteresis TYPE-1 (clockwise) was most common (Fig. 6c), occurring in 8 events, TYPE-2 hysteresis occurred in 1 event, TYPE-3 hysteresis occurred in 5 events, and TYPE-4 hysteresis occurred in 3 events (Fig. 6c).

Stepwise regression on the factor scores versus hysteresis (CONC_DIFF) shows that FACTOR4 with high loadings on peakflow and runoff of the 2nd previous event is negatively correlated, indicating that the 2nd previous event was reducing sediment to the rising limb of the hydrograph or increasing sediment to the falling limb (Table 8). FACTOR3 is significant in the second step of stepwise regression and has high loadings on rainfall to the highest peakflow and rainfall on the falling limb, which are both positively correlated to hysteresis, indicating that as rainfall increases sediment exhaustion increases (Table 8). FACTOR3 also has high loadings on the runoff

Table 8
Results of forward stepwise regression on factor scores for different portions of the hydrograph, Rio Caguitas.

Portion of hydrograph	Response variable	Number of factors used in regression and variance	Significant factor	R^2	P value	Factor Loadings and correlation of explanatory to response variables. A '+' indicates a positive correlation of the explanatory variable(s) to the response variable; a '−' indicates a negative correlation of the explanatory variable(s) to the response variable. See Table 5 for list of abbreviations.
Entire	SED	6:87%	Step 1: Factor3	0.65	0.0001	>0.8(3-PK, 4-MXTMJPK, 5-MXTRP, 6-SMPK)+ <-0.5(25-75LST2)-
			Step 2: Factor5	0.77	0.0039	>0.8(7-TOTRAIN, INT15, 10-RRISE, 11-RAINFOL)+
Entire	CONC	6:88%	Step 1: Factor3	0.44	0.0005	>0.8(3-PK,4-MXTMJPK, 5-MXTRPK, 6-SMPK)+ <-0.5 (25-75LST2)-
			Step 2: Factor6	0.55	0.0388	>0.7 (13-PPTBTW)+
To the highest peak	SEDPK	6:90%	Step 1: Factor3	0.80	0.0001	>0.7(1A-RUNTOPK, 3-PK, 4-MXTMJPK, 10-RRISE)+ <-0.6(25-75LST2)-
To the highest peak	CONCPK	6:90%	Step 1: Factor3	0.51	0.0001	<-0.8(3-PK, 4-MXTMJPK, 10-RRISE)+ <-0.6 (24-INTLST2, 25-75LST2)-
			Step 2: Factor2	0.72	0.0009	>0.8(26-LSPKTI3, 27-SMLSPKT3, 28-RULST3, 29-PPTLSTI3)-
After the highest peak	SEDAFTPK	6:89%	Step 1: Factor4	0.53	0.0001	>0.7(1B-RUNAFTPK,3-PK)+
			Step 2: Factor5	0.71	0.0018	>0.7 (11-RAINFOL)+, <-0.5(12-RNBTWTI)-
After the highest peak	CONCAFTPK	6:90%	Step 1: Factor4	0.28	0.0091	>0.8(11-RAINFOL)+
			Step 2: Factor6	0.47	0.0140	>0.8(13-PPTBTW)+
Hysteresis	CONC_DIFF[a]	6:92%	Step 1: Factor4	0.29	0.0207	>0.8(20-LSPKTI2, 21-SMLSPKTI2,22-RULST2)-
			Step 2: Factor3	0.51	0.0344	>0.7(10-RRISE, 11-RAINFOL)+ <-0.9(12-RNBTWTI)-

[a] The log of CONC_DIFF was used in regression.

since the previous event (12-RNBTWTI) which are negatively correlated to hysteresis indicating that runoff since the previous event is reducing sediment to the rising limb (Table 8).

3.7. Rio Piedras — sediment data

From December 5, 1991 through September 16, 1995, 522 water samples were collected for suspended-sediment concentration at Rio Piedras. Of these samples, 80 were collected during base flow, 168 on the rising limb of the hydrograph to the highest peak, and 274 on the recessional limb of the hydrograph following the 2nd highest peak. Boxplots of the data show the 10th, 25th, 50th, 75th, and 90th percentiles of suspended sediment are 70; 1210; 3280, 7420, and 16,650 mg/L, respectively (Fig. 5a). Rio Piedras had the 2nd highest suspended-sediment concentration to discharge per unit area for any of the four basins, reflecting the higher sediment availability generated from construction activities in this urbanizing basin (Fig. 5b).

For WYs 1991 through 1995, the average suspended-sediment load, sediment yield, and discharge-weighted sediment concentrations were 99,300 Mg, 5120 Mg/km^2/yr, and 6760 mg/L, respectively. For WYs 1991 through 1995, 90% of the average suspended-sediment load was transported in 25 days, 75% in 12 days, and 21% in 1 day.

For the period of study, 280 runoff events occurred, defined by a peakflow over 1.36 m^3/s. Of these runoff events, 26 were sampled adequately to define suspended-sediment load for the entire event (Supplemental Table A.4). Peakflows for the current and past events, with the exception of two events (9/6/1992, 9/6/1995) had recurrence intervals of less than 1.25 years (Supplemental Table A.4).

3.8. Rio Piedras — statistical results

Results of stepwise regression on the factor scores show that factors with high loadings on rainfall, peakflow, and runoff of the current event are positively correlated with the response variables of sediment load and sediment concentration for all three portions of the hydrograph (Table 9). Rainfall since the previous storm event (13-PPTBTW) is negatively correlated to the sediment concentration for the entire event (CONC) and to the highest peakflow (CONCPK) (Table 9).

Hysteresis loops were examined for the 25 sampled events. Hysteresis TYPE-3 is most common (Fig. 6d), occurring in 13 events, TYPE-1 hysteresis occurred in 8 events, TYPE-4 in 3 events, and TYPE-5 in 1 event (Fig. 6d).

Stepwise regression on the factor scores versus hysteresis (CONC_DIFF) shows that FACTOR2 with high loadings on the previous rainfall, peakflow, and runoff is positively correlated to hysteresis. These

results indicate that previous storm events are supplying sediment to the rising limb of the hydrograph.

4. Discussion

4.1. Statistical results

Hydrologic factors controlling storm-generated suspended-sediment loads and concentrations were examined for four basins of differing land use in humid tropical Puerto Rico. For all four study basins, higher R^2 values are observed for the response variables related to sediment loads than for the response variables related to sediment concentration (Tables 6–9). Sediment loads are the product of sediment concentration and discharge, and therefore, there is some spurious correlation of sediment loads to runoff leading to the higher R^2 values (McBean and Al-Nassri, 1988). Hydrologic factors, such as periods of higher rainfall, which lead to higher basinwide soil moisture conditions, can increase runoff (Soler et al., 2008). The higher runoff will increase sediment loads but may not increase sediment availability and sediment concentrations. The higher R^2 values for sediment loads reflect this spurious correlation to discharge and rainfall.

Wetter conditions in the basin are indicated by a higher base flow prior to a runoff event. For example, in the Eastern Pyrenees, Spain, a correlation between antecedent base-flow conditions and runoff was observed (Soler et al., 2008). Base flow is positively correlated with sediment loads for the entire event at Rio Icacos (Fig. 7a; Table 6), where the wetter basin conditions led to higher runoff and higher sediment loads.

For each of the four study basins, the statistical results indicate that rainfall, peakflow, and runoff of the current event are significant in explaining the response variable sediment load and sediment concentration for the entire event, and sediment loads and sediment concentrations before and after the highest peakflow, for all three portions of the hydrograph (Fig. 7a, b, c, and d). Rainfall, peakflow, and runoff of the current event are all positively correlated to the sediment loads and sediment concentrations (Fig. 7a, b, c, and d). In the Eastern Pyrenees, Spain, discharge and rainfall of the current event were important in explaining suspended-sediment concentrations and loads (Rodriguez-Blanco et al., 2010). In the Oregon Coast Range drainages, the rate of hydrograph rise was found to control suspended-sediment concentrations (Beschta, 1987). Higher, fast-rising peakflows in each of the four study basins are a result of high intensity rainfall events that led to rapid runoff with higher sediment loads and sediment concentrations.

Runoff and rainfall since the previous storm event had different relations to sediment loads and concentrations in each of the study

Table 9
Results of forward stepwise regression on factor scores for different portions of the hydrograph, Rio Piedras.

Portion of hydrograph	Response variable	Number of PC's used in regression and variance	Significant factors	R^2	P value	Factor loadings and correlation of explanatory to response variables. A '+' indicates a positive correlation of the explanatory variable(s) to the response variable; a '−' indicates a negative correlation of the explanatory variable(s) to the response variable. See Table 5 for list of abbreviations.
Entire	SED	7:85%	Step 1: Factor3	0.45	0.0002	>0.8(1-RUN, 3-PK, 6-SMPK, 7-TOTRAIN, 10-RRISE)+
Entire	CONC	11:94%	Step 1: Factor11	0.34	0.0018	>0.8(13-PPTBTW)-
			Step 2: Factor1	0.48	0.0227	>0.8(14-LSPKTI, 15-SMLSPKTI, 16-RULST, 17-LSTPPTI, 18-INTLST, 19-75LST)-
To the highest peak	SEDPK	7:87%	Step 1: Factor5	0.49	0.0001	>0.7(1A-RUNTOPK, 3-PK, 10-RRISE)+
To the highest peak	CONCPK	7:88%	Step 1: Factor7	0.19	0.0268	>0.7(4-MXTMJPK)+,<-0.6(13-PPTBTW)-
After the highest peak	SEDAFTPK	7:87%	Step 1: Factor6	0.27	0.0062	>0.7(3-PK,4-MXTMJPK)+
After the highest peak	CONCAFTPK	8:90%	Step 1: Factor1	0.13	0.0700[*]	>0.7(14-LSPKTI, 15-SUMLSPKTI, 16-RULST, 17-LSTPPTI, 18-LSTINT,19-75LST)-
Hysteresis	CONC_DIFF	8:90%	Step 1: Factor2	0.28	0.0171	>0.8(14-LSPKTI, 15-SMLSPKTI, 16-RULST, 17-LSTPPTI, 18-INTLST)+

[*] A variable was not found significant until the p-value equaled 0.07.

basins. At Rio Icacos and Rio Piedras, runoff and rainfall since the previous storm event were reducing sediment that would have been made available for the entire event and to the highest peakflow (Fig. 7a and d; Tables 6 and 9). In Rio Caguitas, precipitation since the previous event was supplying sediment to the entire event leading to TYPE-3 hysteresis (Fig. 7c; Table 8).

In 3 of the study basins (Rio Icacos, Quebrada Blanca, and Rio Piedras), the previous storm event was significant in explaining sediment loads and sediment concentrations of the current event (Fig. 7a, b, and d; Tables 6, 7, and 9). In the basins with limited sediment availability (Rio Icacos and Quebrada Blanca), rainfall, peakflow, and runoff of the previous storm event were supplying sediment, but for different portions of the hydrograph (Fig. 7a and b; Tables 6 and 7). In Rio Icacos, previous event rainfall, peakflow, and runoff supplied sediment to the entire storm hydrograph (Fig. 7a; Table 6). In Quebrada Blanca, previous event peakflow and runoff supplied sediment to the highest peakflow (Fig. 7b; Table 7).

At Rio Piedras, rainfall, peakflow, and runoff of the previous storm event were flushing sediment that would have been available for the entire event and after the highest peakflow (Fig. 7d). Rainfall, peakflow, and runoff of the previous storm event were positively correlated with sediment exhaustion across the hydrograph (TYPE-1 hysteresis). The statistical results for Rio Piedras support a model

where sediment that is normally supplied to the falling limb is removed by previous storm events, leading to TYPE-1 hysteresis

Events further back in time than the previous storm event (2nd previous and 3rd previous events) were significant in explaining sediment loads and sediment concentration in Rio Icacos and Rio Caguitas (Fig. 7a and c). In Rio Icacos, rainfall, runoff, and peak-flow of the 3rd previous storm event increased sediment loads and concentrations to the highest peakflow (Fig. 7a). Higher rainfall and runoff in the 3rd previous storm event may increase basinwide soil moisture conditions, leading to increased runoff and sediment loads in the current event.

For Rio Caguitas, rainfall, peakflow, and runoff of the 2nd and 3rd previous storm events were reducing sediment loads and concentration to the highest peakflow (Fig. 7c). In Rio Caguitas, the majority of the hysteresis loops are clockwise. Sediment from agricultural sources is delivered to the channel during events where it becomes the source of sediment for the next event. TYPE-1 hysteresis is positively correlated with current event rainfall which mobilizes sediment to the rising limb. Previous events may reduce the available sediment from in-channel sources leading to less sediment exhaustion across the hydrograph (TYPE-3 hysteresis) (Fig. 7c). The distance of the agricultural sediment sources may also be an important factor where sediment has to be eroded and delivered to the channel. This
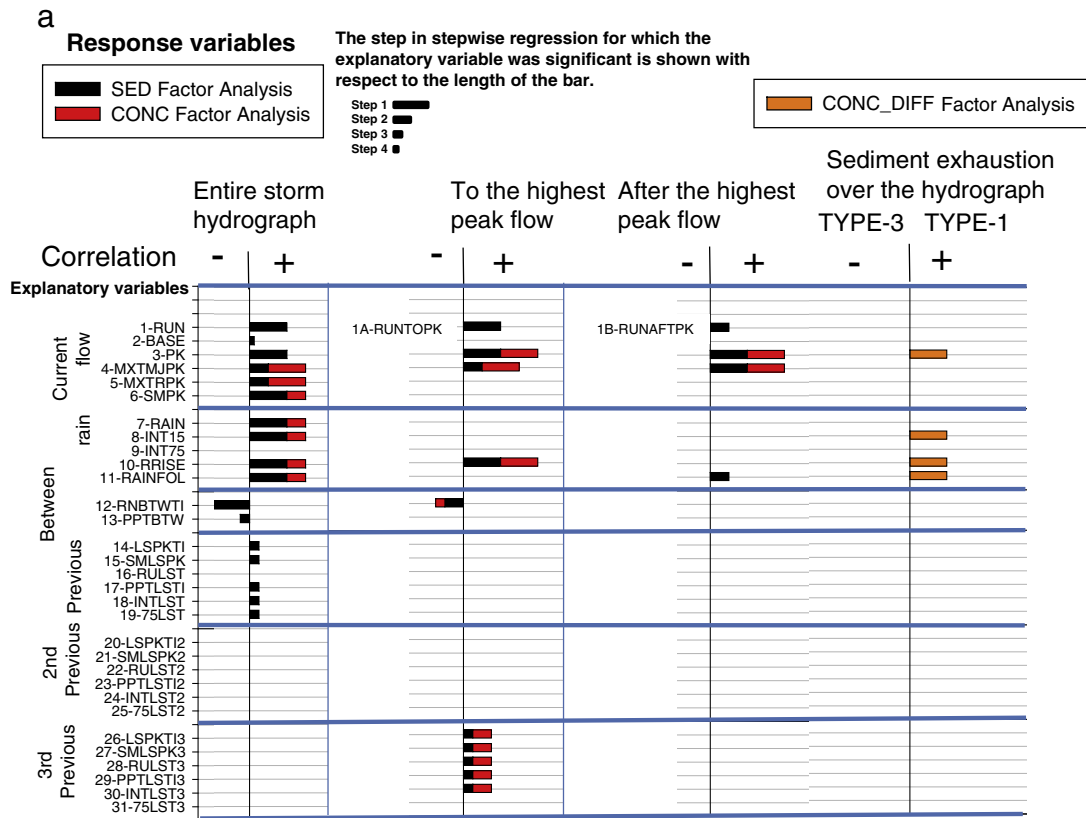
Fig. 7. a. Summary of statistical results of stepwise regression on factor scores of ranked data for Rio Icacos near Naguabo using sediment load (SED), sediment concentration (CONC), and difference of average sediment concentration on the rising limb minus the average sediment concentration on the falling limb (CONC_DIFF) as the response variables. A '+' indicates a positive correlation to the response variables and a '−' indicates a negative correlation. TYPE-1 is clockwise hysteresis, and TYPE-3 is counterclockwise hysteresis. b. Summary of statistical results of stepwise regression on factor scores of ranked data for Quebrada Blanca near El Jagual using sediment load (SED), sediment concentration (CONC), and difference of average sediment concentration on the rising limb minus the average sediment concentration on the falling limb (CONC_DIFF) as the response variables. A '+' indicates a positive correlation to the response variables and a '−' indicates a negative correlation. TYPE-1 is clockwise hysteresis, and TYPE-3 is counterclockwise hysteresis. c. Summary of statistical results of stepwise regression on factor scores of ranked data for Rio Caguitas near Aguas Buenas using sediment load (SED), sediment concentration (CONC), and difference of average sediment concentration on the rising limb minus the average sediment concentration on the falling limb (CONC_DIFF) as the response variables. A '+' indicates a positive correlation to the response variables and a '−' indicates a negative correlation. TYPE-1 is clockwise hysteresis, and TYPE-3 is counterclockwise hysteresis. d. Summary of statistical results of stepwise regression on factor scores of ranked data for Rio Piedras near El Senorial using sediment load (SED), sediment concentration (CONC), and difference of average sediment concentration on the rising limb minus the average sediment concentration on the falling limb (CONC_DIFF) as the response variables. A '+' indicates a positive correlation to the response variables and a '−' indicates a negative correlation. TYPE-1 is clockwise hysteresis, and TYPE-3 is counterclockwise hysteresis.
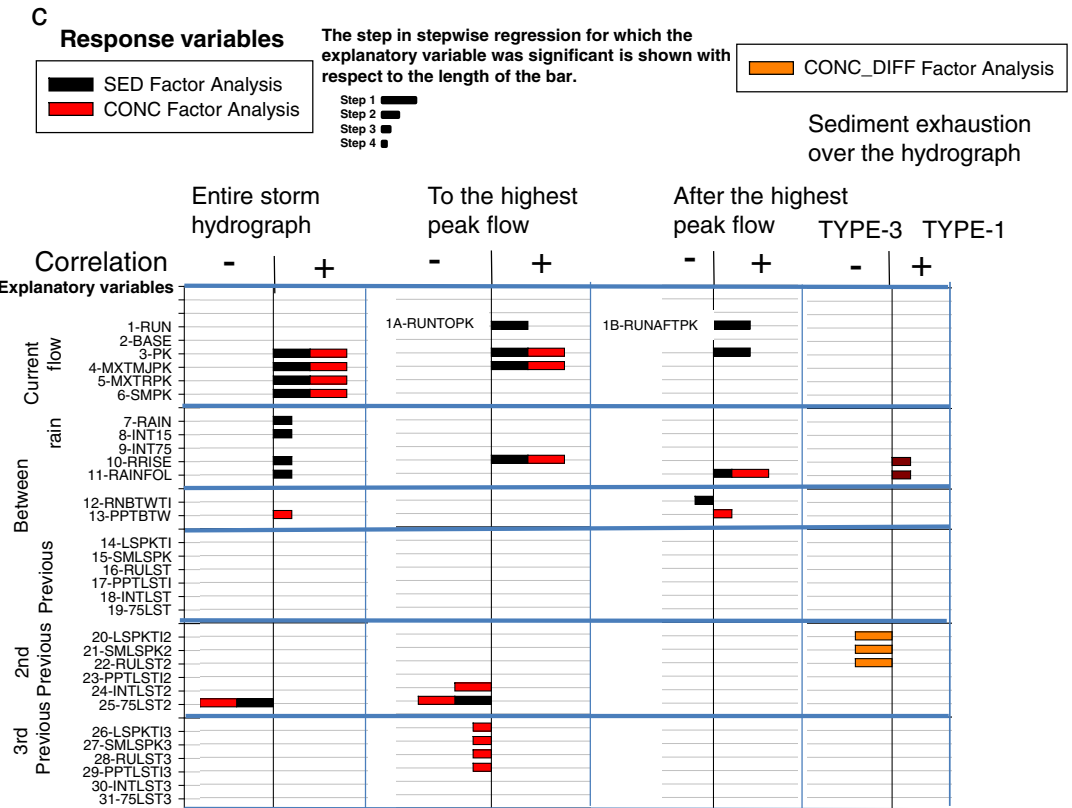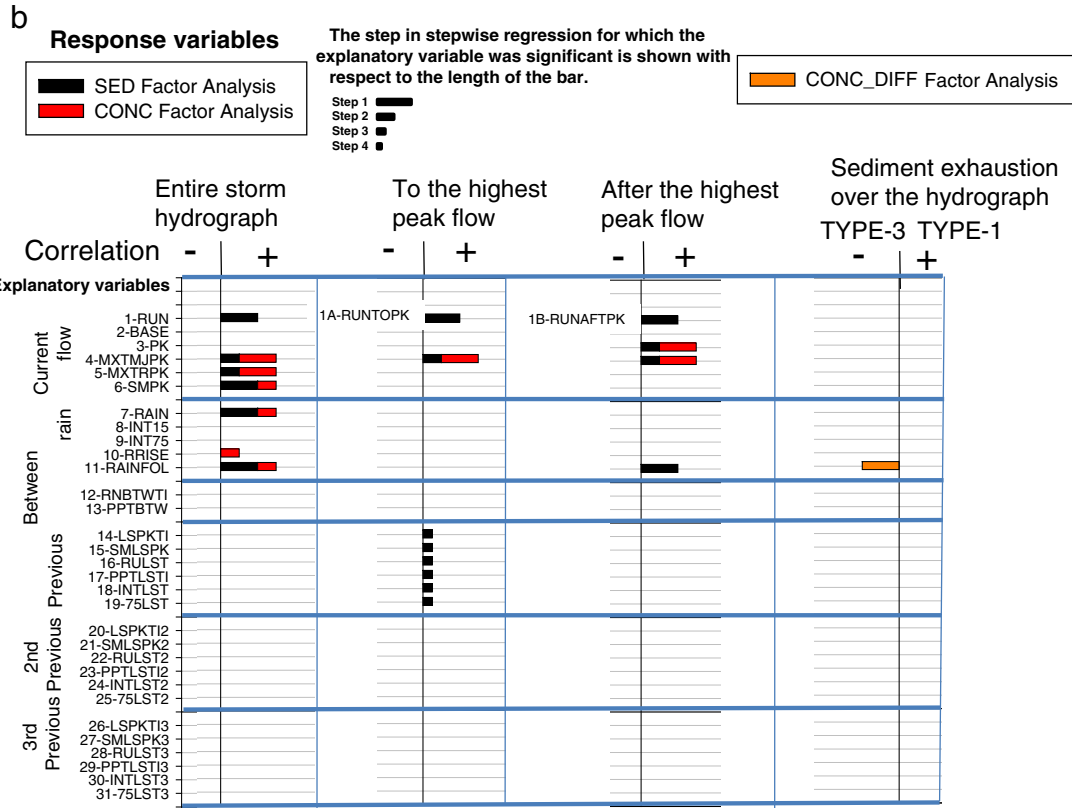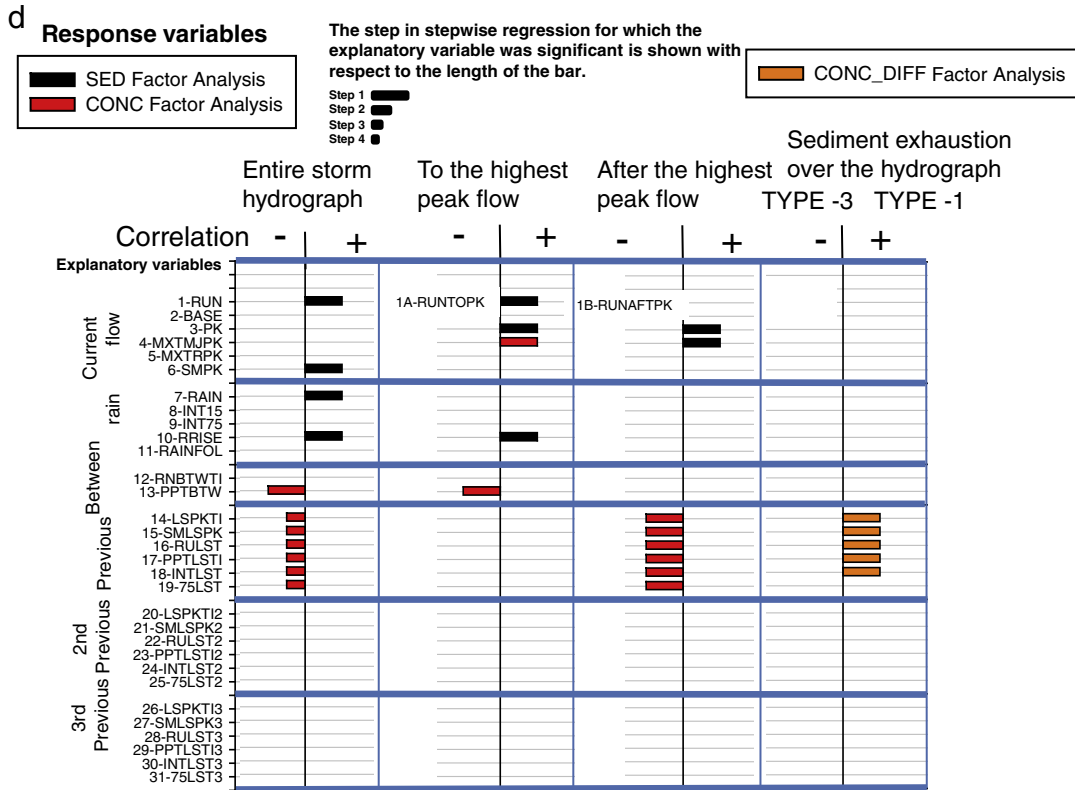
Fig. 7 (*continued*).

Fig. 7 (*continued*).

travel distance and time may cause sediment to reach the sampling station during the recessional portion of the hydrograph, leading to TYPE-3 hysteresis.

4.2. Sediment availability

An objective of this study was to determine if differences in sediment availability between basins influence storm-generated suspended-sediment characteristics. Sediment concentration per unit area of discharge (mg/L:m^3/s/km^2) showed increases with human disturbance in the study basins from the forested Rio Icacos Basin, to the pasture dominated Quebrada Blanca Basin, to the urbanizing Rio Piedras Basin, to the cropland Rio Caguitas Basin, (Fig. 5b). This supports the assumption that land use has a strong control on sediment availability in the study basins.

In all four basins, the dynamics of sediment availability and exhaustion were related to the magnitude and timing of current and past, flow and rainfall events, as well as rainfall and runoff that had occurred since the previous storm event. In the forested Rio Icacos Basin of limited sediment availability, storms with higher rainfall, higher runoff, and steep-rising peakflows transport greater suspended-sediment loads, and have higher sediment concentration for the entire event (Fig. 7a). In Rio Icacos the majority of the storms (79%) showed clockwise (TYPE-1) hysteresis (Fig. 6a). Sadeghi et al. (2008) documented TYPE-1 hysteresis loops in the 4.8-ha Hinotani-ike forested watershed in Japan. In this reforested watershed, TYPE-1 hysteresis loops and the reduction in suspended-sediment concentration over the hydrograph were associated with sediment availability, rainfall, soil water repellency, and different flow components (Sadeghi et al., 2008). In Rio Icacos, sediment is supplied to the channel by the previous storm and the 3rd previous storm event. High rainfall with higher runoff on the rising limb, and steep-rising peakflows mobilizes in-channel sources of

sediment to the rising limb of the hydrograph, and clockwise hysteresis occurs. During the study period, Rio Icacos had a fine-sand bed with a median particle diameter of 0.6 mm, where sediment was mobilized at most flows (Larsen, 1997). Higher rainfall and runoff that occurred since the previous storm event flushed this in-channel sediment from the system, leading to lower sediment loads and sediment concentrations on the rising limb of the hydrograph. The lower amounts of sediment on the rising limb led to less sediment exhaustion across the storm hydrograph (Fig. 7a). Wetter periods in Rio Icacos led to higher base flow and increased runoff and sediment loads for the entire event and after the highest peakflow (Fig. 7a).

In the pasture dominated Quebrada Blanca Basin with limited sediment availability from cropland, storms with higher rainfall, higher runoff, and fast rising peakflows transport greater suspended-sediment loads and have higher sediment concentrations (Fig. 7b). TYPE-1 hysteresis loops are most common, occurring in 59% of the storm events (Fig. 6b). In Quebrada Blanca, previous events supplied sediment to the channel where it becomes a source of sediment to the rising limb of the storm hydrograph (Fig. 7b). Higher rainfall events on the falling limb supplied sediment to the recessional limb and TYPE-3 hysteresis occurred.

In the agricultural Rio Caguitas Basin with high sediment availability, sediment loads and concentrations for the entire event increased with flow and rainfall factors of the current event (Fig. 7c). TYPE-1 hysteresis loops were most common, occurring in 47% of the events (Fig. 6c). Sediment that is delivered to a channel by previous events can be the source of sediment to the current event rising flow, resulting in TYPE-1 hysteresis (Smith and Dragovich, 2009; Wood, 1977). In Rio Caguitas, cropland is a distant source of sediment relative to the channel and the sediment mobilized from previous storms may be deposited in the channel. This deposited sediment becomes the source of sediment to the rising limb of the next event and TYPE-1 hysteresis occurs.

In Rio Caguitas, TYPE-3 hysteresis may be a result of several conditions. Counterclockwise loops indicate a distance source of sediment (Klein, 1984), where sediment arrived after the highest peakflow. In Rio Caguitas, the agricultural areas were the distant source of sediment. Another process leading to TYPE-3 hysteresis was the flushing of in-channel sediment by previous events (2nd and 3rd previous storm events) that would have been available to the rising limb thus reducing available to the rising limb resulting in less sediment depletion across the hydrograph.

In the urbanizing Rio Piedras Basin of high sediment availability, storms with high rainfall and high runoff that have steep rising peakflows increased suspended-sediment loads in the current event (Fig. 7d). TYPE-3 hysteresis loops were most common, occurring in 52% of the events. In Rio Piedras, the occurrence of TYPE-3 hysteresis loops was consistent with other studies that showed TYPE-3 hysteresis when the sediment sources are from distant portions in the basins (Table 1). In Rio Piedras, the distant sediment sources were the active construction sites that were present in the upper portions of the basin during this study (Fig. 3f). Sediment from the construction sites arrived to the stream after the highest peakflow leading to TYPE-3 hysteresis. Another component influencing Type-3 hysteresis in Rio Piedras is the elaborate network of stormwater runoff features found in this urban basin (Lugo et al., 2011). Stormwater runoff transports little sediment and can reach the channel early in the event before the upland sediment source arrives, leading to lower suspended-sediment concentrations on the rising limb and Type-3 hysteresis.

In Rio Piedras, previous storm events were correlated with lower sediment concentrations for the current event, and greater sediment exhaustion across the hydrograph (TYPE-1 hysteresis) (Fig. 7d). Large previous event, runoff and rainfall factors increased sediment to the rising limb of the hydrograph and/or removed available sediment to the recessional limb (Fig. 7d). In Rio Piedras, the higher percentage of TYPE-3 hysteresis indicates that most storms deliver sediment to the recessional limb of the hydrograph. Some of this sediment may be deposited in the channel where it becomes a source of sediment to the next event rising limb. Larger previous storms supply more sediment to the channel. Stormwater runoff which arrives early in the event would mobilize the sediment in channel storage leading to TYPE-1 hysteresis. Large previous storm events may also be depleting easily eroded sediment from construction sites, leading to less available sediment on the recessional limb. In Rio Piedras, rainfall between events flushed sediment from the system, leading to lower sediment loads and concentrations in the current event (Fig. 7d). The large impervious surface area in Rio Piedras would favor runoff from small, localized rains removing sediment from channel storage.

The location of sediment sources in each basin has an effect on sediment delivery to the channel and to the sampling station. Many factors influence sediment delivery including rainfall, runoff, vegetation density and type, slope, soil properties, drainage density, and the relief to length ratio, where length is defined as the distance to the nearest channel (Lu et al., 2003; Roehl, 1962). The forested and pasture basins may deliver some upland sediment to the channel where it is deposited, and it becomes an in-channel source of sediment for the next event. These in-channel sources of sediment can be delivered rapidly to the sampling station on the rising limb of the storm hydrograph resulting in TYPE-1 hysteresis. Distant channel sources (agriculture and construction) have to be delivered to the channel system and then transported to the sampling station. For both the agricultural and urbanizing basins, some of the sediment may reach the sampling station on the recessional portion of the hydrograph and some sediment may be deposited in the channel. Because a majority of the urbanizing basin is impervious, sediment delivery is more efficient than in the agricultural basin, where vegetation cover is higher. In the urbanizing basin, a large majority of the storms are counterclockwise (TYPE-3 hysteresis), demonstrating that much of the sediment reaches the sampling station on the recessional limb.

A model of sediment transport in humid-tropical Puerto Rico was developed from the statistical interpretations of the four study basins (Fig. 8). In sediment-limited, relatively undisturbed forested basins, storm events supply sediment to the channel (Fig. 8). Rainfall and runoff events that occur between storms flush this sediment from channel storage. In urbanizing basins where upland land use is an important source of sediment, storms flush sediment from the system (Fig. 8). Sediment availability increases between storm events from human disturbances, such as construction activities (Fig. 8). As a basin proceeds from an undisturbed to a disturbed state, storm-generated hysteresis loops change from clockwise (TYPE-1) to counterclockwise (TYPE-3) hysteresis loops (Fig. 9) as sediment is derived from distant portions of the basin.

The statistical approaches developed in this paper can be used to generate hypotheses and improve field studies designed to understand sediment processes. For example, the recognition of in-channel sediment as an important source of sediment in this study could be verified using sediment fingerprinting approaches (Collins et al., 2010; Gellis and Walling, 2011). Samples taken of in-channel sediment can be analyzed to determine their sources. Subsequent sampling of rising limb and falling limb flows can be used to determine if the sources across the hydrograph are from these in-channel sources or upland sources.

5. Conclusions

Sediment availability, expressed as sediment concentration per unit discharge, increased with human disturbance in the four study basins from the forested Rio Icacos Basin, to the pasture-dominated Quebrada Blanca Basin, to the urbanizing Rio Piedras Basin, and to the cropland Rio Caguitas Basin. One-hundred and twenty moderate storms with recurrence intervals generally less than 1.25 years were examined for the four basins. For each basin, current event hydrologic characteristics of flow, peakflow, rainfall, and rates of peak-flow rise were significant in explaining storm-generated sediment loads and sediment concentrations for all portions of the hydrograph (for the entire event, to the highest peakflow, and after the highest peakflow).

Both sediment loads and sediment concentrations were used as response variables in this study. Because sediment loads are computed as a product of discharge and sediment concentration, increases in storm-generated sediment loads can be a result of higher runoff but not necessarily concomitant with increasing sediment availability.
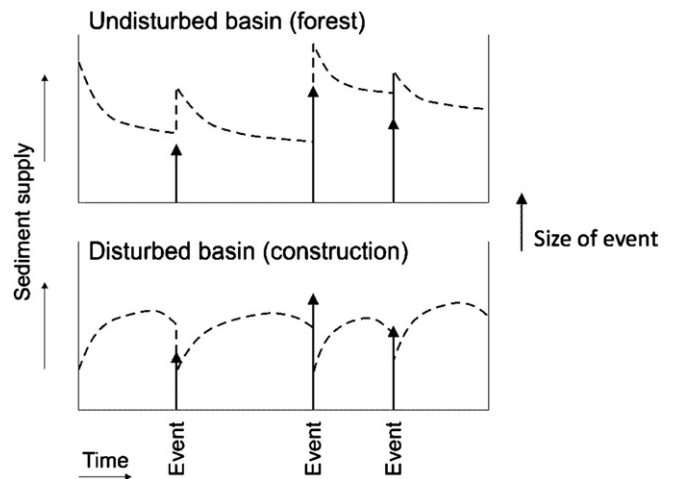

Fig. 8. Model showing the effect of storm events and runoff between storm events on generating or reducing available sediment in basins with low sediment availability (forested) and high sediment availability (urbanizing). In the forested basin, events generate sediment where it is deposited in the channel and removed by runoff between events. In the urbanizing basin, events flush sediment from the system and construction activities between events build up sediment availability.
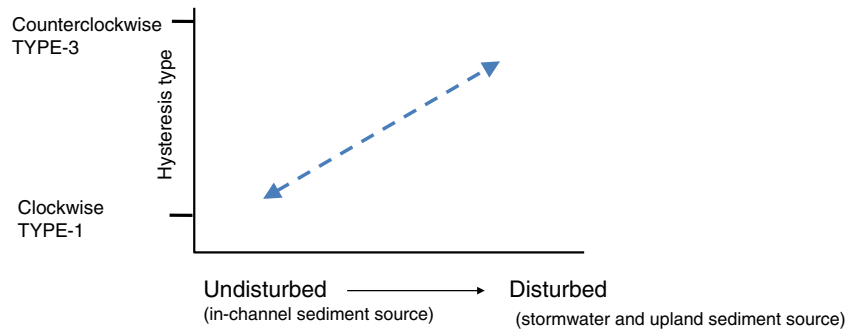
Fig. 9. Relation of basin disturbance to hysteresis type. Clockwise hysteresis loops are related to in-channel sediment sources and counterclockwise hysteresis loops are related to stormwater runoff delivering low suspended-sediment concentrations to the rising limb of the hydrograph and distance sources of sediment delivered on the hydrograph recession.

Circumstances that could increase runoff and not sediment concentrations include wetter periods which increase soil moisture leading to higher runoff, but not necessarily greater sediment detachment. The statistical interpretations presented here cannot easily distinguish whether higher runoff or higher sediment availability controls sediment loadings.

Results from this study indicate that sediment availability affects how the timing and magnitude of runoff, peakflow, and rainfall events affect sediment loads, sediment concentrations, and hysteresis type. In the undisturbed forested basin (Rio Icacos) and pasture basin (Quebrada Blanca), large events mobilize and supply sediment to the channel. If the next event is closely spaced in time, this channel sediment becomes the source of sediment to the rising limb of the hydrograph and clockwise hysteresis (TYPE-1) occurs. Moderate storm events that occur between events in the forested basin flush the channel sediment from the fluvial system, leading to lower sediment concentrations and less sediment exhaustion across the hydrograph. Lithology can also be an important factor controlling sediment transport. In the forested Rio Icacos Basin, which is underlain by intrusive rocks that weather to a fine sand, the bed sediment (0.6 mm) is readily mobilized between events, and can lower the available sediment for the next event.

In the disturbed urbanizing basin, construction sites were the main source of sediment. Sediment is eroded from these distant sources and delivered to the streamflow-gaging station on the recessional limb of the current storm hydrograph and counterclockwise hysteresis (TYPE-3) occurred. Stormwater runoff which arrives early in the event with low suspended-sediment concentrations also contributes to hydrographs with TYPE-3 hysteresis. Some of the sediment transported on the falling limb during large storms is deposited in the channel. The deposited sediment becomes a source of sediment for the next event on the rising limb and TYPE-1 hysteresis occurred. Large storm events also depleted easily eroded sediment from construction sites, causing the next event to have lower sediment loads and sediment concentrations. Since most of the sediment in the disturbed basin is delivered on the recessional limb, the reduced amount of sediment supplied from previous storms led to less available sediment on the recessional limb and clockwise hysteresis occurred (TYPE-1). The high impervious surface area in the Rio Piedras Basin leads to rainfall between events flushing sediment from channel storage.

The transport of storm-derived sediment in the four Puerto Rican streams supports a concept of sediment availability and transport that is described in the literature, where clockwise hysteresis loops are common when sediment is supplied by in-channel or near channel sources and counterclockwise hysteresis loops occur when sediment is derived from distant basin sources or by the depletion of channel sediment that would have been available to the rising portion of the hydrograph.

A model of sediment availability and hysteresis for humid-tropical Puerto Rico was developed from this study. As sediment availability increases in a basin, hysteresis loops change from clockwise (TYPE-1) to counterclockwise (TYPE-3), indicating a shift from channel sources to upland sources, which are in distant portions of the basin and have longer travel times. Storm events in basins with less sediment availability, such as forested basins, increase the supply of sediment to the channel and smaller storms between events flush this sediment. In basins with greater sediment availability, storm events flush sediment from the hillslopes and channels. The statistical approaches developed in this paper can be used to generate hypotheses and improve field studies designed to understand sediment processes.

Supplementary data to this article can be found online at http://dx.doi.org/10.1016/j.catena.2012.10.018.

Acknowledgments

References

Asselman, N.E.M., 1999. Suspended sediment dynamics in a large drainage basin—the River Rhine. Hydrological Processes 13, 1437–1450.

Baca, P., 2008. Hysteresis effect in suspended sediment concentration in the Rybarik basin, Slovakia. Hydrological Processes 53, 224–235.

Baxter, M.J., 1995. Standardization and transformation in principal component analysis, with applications to archaeometry. Journal of the Royal Statistical Society, Series C 44 (4), 513–527.

Beschta, R.L., 1987. Conceptual models of sediment transport in streams. In: Thorne, C.R., Bathurst, J.C., Hey, R.D. (Eds.), Sediment Transport in Gravel-Bed Rivers. John Wiley, Chichester, UK, pp. 387–419.

Boccheciamp, R.A., 1977. Soil Survey of Humacao Area of Eastern Puerto Rico. U.S. Department of Agriculture, Soil Conservation Service . 103 pp.

Boccheciamp, R.A., 1978. Soil Survey of San Juan area of Puerto Rico. U.S. Department of Agriculture, Soil Conservation Service. 141 pp.

Brasington, J., Richards, K., 2000. Turbidity and suspended sediment dynamics in small catchments in the Nepal Middle Hills. Hydrological Processes 14, 2559–2574.

Briggs, R.P., Akers, J.P., 1965. Hydrogeologic map of Puerto Rico and adjacent islands. Hydrologic Investigations Atlas HA-197, U.S. Geological Survey, scale 1:240,000.

Bull, L.J., Lawler, D.M., Leeks, G.J.L., Marks, S., 1995. Downstream changes in suspended sediment fluxes in the River Severn, UK. In: Osterkamp, W.R. (Ed.), Effects of Scale on Interpretation and Management of Sediment and Water Quality: Proceedings of the Boulder Symposium, July, 1995, International Association of Hydrological Sciences Publication no. 226, pp. 27–37.

Cattell, R.B., 1966. The scree test for the number of factors. Multivariate Behavioral Research 1 (2), 245–276.

Collins, A.L., Walling, D.E., Webb, L., King, P., 2010. Apportioning catchment scale sediment sources using a modified composite fingerprinting technique incorporating property weightings and prior information. Geoderma 155, 249–261.

Costa, J.E., 1977. Sediment concentration and duration in stream channels. Journal of Soil and Water Conservation 32, 168–170.

Daultrey, S., 1976. Principal components analysis. Concepts and Techniques in Modern Geography, 8. Institute of British Geographers, pp. 1–51.

Davis, J.C., 1986. Statistics and Data Analysis in Geology. John Wiley, NY.

Donnelly, T.W., 1989. Geologic history of the Caribbean and Central America. In: Bally, A.W., Palmer, A.R. (Eds.), The Geology of North America—An Overview. Geological Society of America, Boulder Colorado, pp. 299–321.

Douglas, I., Guyot, J.L., 2004. Erosion and sediment yield in the humid tropics. In: Bonell, M., Bruijnzeel, L.A. (Eds.), Forest, Water and People in the Humid Tropics. International Hydrology Series. Cambridge University Press, Cambridge, pp. 407–421. ch. 15.

Dunne, T., 1979. Sediment yield and land use in tropical catchments. Journal of Hydrology 42, 281–300.

Duvert, C., et al., 2010. Drivers of erosion and suspended sediment transport in three headwater catchments of the Mexican Central Highlands. Geomorphology 123 (3–4), 243–256.

Eder, A., Strauss, P., Krueger, T., Quinton, J.N., 2010. Comparative calculation of suspended sediment loads with respect to hysteresis effects (in the Petzenkirchen catchment, Austria). Journal of Hydrology 389, 168–176.

Edwards, T.K., Glysson, G.D., 1988. Field methods for measurement of fluvial sediment. U.S. Geological Survey Open-File Report 86-531, pp. 1–118.

Gellis, A.C., 1991. Construction effects on sediment for two basins, Puerto Rico. Proceedings of the Fifth Federal Interagency Sedimentation Conference, pp. 72–78. Chapter 4, Las Vegas, Nevada.

Gellis, A.C., 2003. Suspended-sediment characteristics in four humid tropical watersheds of contrasting land use, Puerto Rico. Colorado State University, Unpublished Ph.D dissertation.

Gellis, A.C., Walling, D.E., 2011. Sediment-source fingerprinting (tracing) and sediment budgets as tools in targeting river and watershed restoration programs. In: Simon, A., Bennett, S., Castro, J.M. (Eds.), Stream Restoration in Dynamic Fluvial Systems: Scientific Approaches, Analyses, and Tools: American Geophysical Union Monograph Series, 194, pp. 263–291.

Gellis, A.C., Webb, R.M.T., Wolfe, W.J., McIntyre, S.C.I., 1999. Effects of land use on upland erosion, sediment transport, and reservoir sedimentation, Lago Loiza Basin, Puerto Rico. U.S. Geological Survey Water-Resources Investigations Report 99-4010, pp. 1–60.

Gellis, A.C., Webb, R.M.T., Wolfe, W.J., McIntyre, S.C.I., 2006. Changes in land use and reservoir sedimentation–a case study in the Lago Loiza basin, Puerto Rico. Physical Geography 27, 39–69.

Gellis, A.C., Hupp, C.R., Pavich, M.J., Landwehr, J.M., Banks, W.S.L., Hubbard, B.E., Langland, M.J., Ritchie, J.C., Reuter, J.M., 2009. Sources, transport, and storage of sediment at selected sites in the Chesapeake Bay watershed. U.S. Geological Survey Scientific Investigations Report 2008-5186, pp. 1–95.

Glysson, G. Douglas, 1987. Sediment-transport curves. U.S. Geological Survey Open-File Report 87-218, pp. 1–47.

Godfrey, A.E., Everitta, B.L., Duqueb, J.F.M., 2008. Episodic sediment delivery and landscape connectivity in the Mancos Shale badlands and Fremont River system, Utah, USA. Geomorphology 102, 242–251.

Goodwin, P., Denton, R.A., 1991. Seasonal influences on the sediment transport characteristics of the Sacramento River, California. Proceedings of the Institution of Civil Engineers, Part 2. Research and Theory 91, 163–172.

Guy, H.P., 1964. An analysis of some storm-period variables affecting stream sediment transport. U.S. Geological Survey Professional Paper 462-E, pp. 1–46.

Guy, H.P., 1969. Laboratory theory and methods for sediment analysis. U.S. Geological Survey Techniques of Water Resources Investigations, Book, 5, pp. 1–58. Chap. C1.

Heidel, S.G., 1956. The progressive lag of sediment concentration with flood waves. Transactions American Geophysical Union 37, 56–66.

Heywood, R.B., Dartnall, H.J.G., Priddle, J., 1980. Characteristics and classification of the lakes of Signy Island, South Orkney Islands, Antarctica. Freshwater Biology 10, 47–59.

Hooke, Roger LeB., 2000. On the history of humans as geomorphic agents. Geology 28 (9), 843–846.

Horowitz, A.J., 2008. Determining annual suspended sediment and sediment-associated trace element and nutrient fluxes. Science of the Total Environment 400 (1–3), 315–343.

Hughes-Hallett, D., 1994. Calculus. John Wiley and Sons.

Jibson, R.W., 1989. Debris flows in southern Puerto Rico. Geological Society of America Special Paper 236, 29–55.

Kaiser, H.F., 1960. The application of electronic computers to factor analysis. Educational and Psychological Measurement 20, 141–151.

Kattan, Z., Gac., J.Y., Probst, J.L., 1987. Suspended sediment load and mechanical erosion in the Senegal Basin — estimation of the surface runoff concentration and relative contributions of channel and slope erosion. Journal of Hydrology 92, 59–76.

Kennedy, W.J., 1984. Discharge ratings at gaging stations. U.S. Geological Survey Techniques of Water-Resources Investigations, Book, 3. Chap. A1, 58 pp.

Klein, M., 1984. Anticlockwise hysteresis in suspended sediment concentration during individual storms — Holbeck Catchment, England. Catena 11, 251–257.

Krishnaswamy, J., Richter, D.D., Halpin, P.N., Hofmockel, M.S., 2001. Spatial patterns of suspended-sediment yields in a humid tropical watershed in Costa Rica. Hydrological Processes 15, 2237–2257.

Kurashige, Y., 1994. Mechanisms of sediment supply in headwater rivers. Transactions, Japanese Geomorphological Union 15A, 109–129.

Larsen, M.C., 1997. Tropical geomorphology and geomorphic work–A study of geomorphic processes and sediment and water budgets in montane humid-tropical forested and developed watersheds, Puerto Rico. Unpublished Ph.D. dissertation, University of Colorado, 341 pp.

Larsen, M.C., 2012. Landslides and sediment budgets in four watersheds in Eastern Puerto Rico. In: Murphy, S.F., Stallard, R.F. (Eds.), Water Quality and Landscape Processes of Four Watersheds in Eastern Puerto Rico: U.S. Geological Survey Professional Paper 1789, pp. 113–152. Chapter F.

Larsen, M.C., Santiago-Roman, A., 2001. Mass wasting and sediment storage in a small montane watershed: an extreme case of anthropogenic disturbance in the humid tropics. In: Dorava, J.M., Fitzpatrick, F., Palcsak, B.B., Montgomery, D.R. (Eds.), Geomorphic Processes and Riverine Habitat: American Geophysical Union Monograph, pp. 142–170.

Larsen, M.C., Simon, A., 1993. Rainfall-threshold conditions for landslides in a humid-tropical system, Puerto Rico. Geografiska Annaler 75A (1–2), 13–23.

Larsen, M.C., Stallard, R.F., 2000. Water, energy, and biogeochemical budgets Luquillo Mountains, Puerto Rico. U.S. Geological Survey Fact Sheet, FS 163-99. 4 pp.

Larsen, M.C., Torres Sánchez, A.J., 1998. The frequency and distribution of recent landslides in three montane tropical regions of Puerto Rico. Geomorphology 24 (4), 309–331.

Larsen, M.C., Torres-Sanchez, A.J., 1992. Landslides triggered by Hurricane Hugo in eastern Puerto Rico, September 1989. Caribbean Journal of Science 28, 113–125.

Larsen, M.C., Webb, R.M.T., 2009. Potential effects of runoff, fluvial sediment, and nutrient discharges on the coral reefs of Puerto Rico. Journal of Coastal Research 25 (1), 189–208.

Larsen, M.C., Gellis, A.C., Glysson, G.D., Gray, J.R., Horowitz, A.J., 2010. Fluvial sediment in the environment: a national problem. Proceedings, 2nd Joint Federal Interagency Conference, Las Vegas, NV. June 27–July 1, 2010 (15 pp.).

Leopold, L.B., 1956. Land Use and Sediment Yield. In: Thomas Jr., W.L. (Ed.), Man's Role in Changing the Face of the Earth. University of Chicago Press, Chicago, pp. 639–647.

Lewis, L.A., 1974. Slow movement of earth under tropical rainforest conditions. Geology 2, 9–10.

Lewis, J.F., Draper, G., 1990. Geology and tectonic evolution of the northern Caribbean margin. In: Dengo, G., Case, J.E. (Eds.), The Caribbean Region. The Geology of North America, vol. H. Geological Society of America, pp. 77–140.

Loughran, R.J., 1977. Sediment transport from a rural catchment in New South Wales R.J. Journal of Hydrology 34, 357–375.

Loughran, R.J., Campbell, B.L., Elliott, G.L., 1986. Sediment dynamics in a partially cultivated catchment in New South Wales, Australia. Journal of Hydrology 83, 285–297.

Lu, H., Moran, C.J., Prosser, I.P., Raupach, M.R., Olley, J., Petheram, C., 2003. Sheet and rill erosion and sediment delivery to streams—a basin wide estimation at hillslope to medium catchment scale. Land and Water, Technical Report 15/03. Australian Commonwealth Scientific & Industrial Research Organization (CSIRO). 56 pp.

Lugo, A.E., Ramos, O., Rodriguez-Pedraza, C., 2011. The Río Piedras Watershed and Its Surrounding Environment FS-980 U.S. Department of Agriculture, Forest Service, International Institute of Tropical Forestry. 46 pp.

Marcus, W.A., 1989. Lag-time routing of suspended-sediment concentrations during unsteady flow. Bulletin of the Geological Society of America 101, 644–651.

McBean, E.A., Al-Nassri, S., 1988. Uncertainty in suspended sediment transport curves. Journal of Hydraulic Engineering 114 (1), 63–74.

Monroe, W.H., 1980. Geology of the middle tertiary formations of Puerto Rico. U.S. Geological Survey Professional Paper 953. 93 pp.

Moore, R.J., 1984. A dynamic model of basin sediment yield. Water Resources Research 20, 89–103.

Pease, M.H., 1968. Geologic map of the Aguas Buenas quadrangle, Puerto Rico. U.S. Geological Survey Miscellaneous Geologic Investigations Map I-479.

Picouet, C., Hingray, B., Olivry, J.C., 2001. Empirical and conceptual modeling of the suspended sediment dynamics in a large tropical African river—the Upper Niger basin. Journal of Hydrology 250, 19–39.

Porterfield, G., 1972. Computation of fluvial-sediment discharge. U.S. Geological Survey Techniques of Water-Resources Investigations Book 3. Chapter C3, 66 pp.

Reid, M.K., Spencer, K.L., 2009. Use of principal components analysis (PCA) on estuarine sediment datasets — the effect of data pre-treatment. Environmental Pollution 157 (8–9), 2275–2281.

Rieger, W.A., Olive, L.J., 1986. Sediment responses during storm events in small forested watersheds. In: El-Shaarawi, A.H., Kwiatkowski, R.E. (Eds.), Proceedings of the Workshop held at the Canada Centre for Inland Waters, October 7–10, 1985, Burlington, Ontario, Canada, pp. 490–497.

Rinaldi, M., Casagli, N., Dapporto, S., Gargini, A., 2004. Monitoring and modeling of pore water pressure changes and riverbank stability during flow events. Earth Surface Processes and Landforms 29 (2), 237–254.

Rodríguez-Blanco, M.L., Taboada-Castro, M.M., Taboada-Castro, M.T., 2010. Factors controlling hydro-sedimentary response during runoff events in a rural catchment in the humid Spanish zone. Catena 82, 206–217.

Roehl, J.E., 1962. Sediment source areas, delivery ratios, and influencing morphologic factors. International Association of Hydrological Sciences Publication 59, 202–213.

Sadeghi, S.H.R., Mizuyama, T., Miyata, S., Gomi, T., Kosugi, K., Fukushima, T., Mizugaki, S., Onda, Y., 2008. Determinant factors of sediment graphs and rating loops in a reforested watershed. Journal of Hydrology 356, 271–282.

Scatena, F.N., Larsen, M.C., 1991. Physical aspects of Hurricane Hugo in Puerto Rico. Biotropica 23 (4a), 317–323.

Seeger, M., Errea, M.P., Begueria, S., Marti, C., Garzia-Ruiz, J.M., Arnaez, J., 2004. Catchment soil moisture and rainfall characteristics as determinant factors for discharge/suspended sediment hysteretic loops in a small headwater catchment in the Spanish Pyrenees. Journal of Hydrology 288, 299–311.

Shanley, J.B., McDowell, W.H., Stallard, R.F., 2011. Long-term patterns and short-term dynamics of stream solutes and suspended sediment in a rapidly weathering tropical watershed. Water Resources Research 47, W07515. http://dx.doi.org/10.1029/2010WR009788 11 pp.

Sharma, K.D., Dhir, R.P., Murthy, J.S.R., 1992. Modelling sediment transport in arid upland basins in India. International Association of Hydrological Sciences Publication 209, 169–176.

Sidle, R.C., Campbell, A.J., 1985. Patterns of suspended-sediment transport in a coastal Alaska stream. Water Resources Bulletin 21, 909–917.

Sidle, R.C., Ziegler, A.D., Negishi, J.N., Abdul Rahim, N., Siew, R., Turkelboom, F., 2006. Erosion processes in steep terrain—truths, myths, and uncertainties related to forest management in Southeast Asia. Forest Ecology and Management 224, 199–225.

Simon, A., Larsen, M.C., Hupp, C.R., 1990. The role of soil processes in determining mechanisms of slope failure and hillslope development in a humid-tropical forest, eastern Puerto Rico. Geomorphology 3, 263–286.

Simon, A., Curini, A., Darby, S., Langendoen, E.J., 2000. Bank and near-bank processes in an incised channel. Geomorphology 35, 193–217.

Skoklevski, Z., Velickov, S., 1995. Total suspended load transport as a natural stochastic process: effects of scale on interpretation and management of sediment and water quality. proceedings of the boulder symposium, July 1995. International Association of Hydrological Sciences Publication 226, 215–221.

Smith, H.G., Dragovich, D., 2009. Interpreting sediment delivery processes using suspended sediment-discharge hysteresis patterns from nested upland catchments, south-eastern Australia. Hydrological Processes 23, 2415–2426.

Soler, M., Latron, J., Gallart, F., 2008. Relationships between suspended sediment concentrations and discharge in two small research basins in a mountainous Mediterranean area (Vallcebre, Eastern Pyrenees). Geomorphology 98 (1–2), 143–152.

Stallard, R.F., Murphy, S.F., 2012. Water quality and mass transport in four watersheds in Puerto Rico. In: Murphy, S.F., Stallard, R.F. (Eds.), Water Quality and Landscape Processes of Four Watersheds in Eastern Puerto Rico: U.S. Geological Survey Professional Paper 1789, pp. 113–152. Chapter E.

Statistical Analysis System (SAS), 1989. SAS Institute Inc., Cary, North Carolina.

Syvitski, J.P.M., Kettner, A., 2011. Sediment flux and the Anthropocene. Philosophical Transactions of the Royal Society A–Mathematical, Physical and Engineering Sciences 369, 957–975.

VanSickle, J., Beschta, R.L., 1983. Supply-based models of suspended sediment transport in streams. Water Resources Research 19, 768–778.

Walling, D.E., 1974. Suspended sediment and solute yields from a small catchment prior to urbanization. In: Gregory, K.J., Walling, D.E. (Eds.), Fluvial Processes in Instrumented Watersheds: Institute of British Geographers Special Publication No. 6, pp. 169–192.

Walling, D.E., Webb, B.W., 1982. Sediment availability and the prediction of storm-period sediment yields. International Association of Hydrological Sciences Publication 137, 327–337.

Wang, Y., Ren, M., Syvitski, J.P.M., 1998. Sediment transport and terrigenous flux. In: Brink, K.H., Robinson, A.R. (Eds.), The Sea, Volume 10, The Global Coastal Ocean. John Wiley and Sons, pp. 253–292.

Warne, A.G., Webb, R.M.T., Larsen, M.C., 2005. Water, sediment, and nutrient discharge characteristics of Puerto Rico rivers and their potential influence on coral reefs. U.S. Geological Survey Scientific Investigations Report 2005-5206. 58 pp.

White, A.F., Blum, A.E., Schulz, M.S., Vivit, D.V., Stonestrom, D.A., Larsen, M., Murphy, S.F., Eberl, D., 1998. Chemical weathering in a tropical watershed, Luquillo Mountains, Puerto Rico: I. Long-term versus short-term weathering fluxes. Geochimica et Cosmochimica Acta 62 (2), 209–226.

Williams, G.P., 1989. Sediment concentration versus water discharge during single hydrologic events. Journal of Hydrology 111, 89–106.

Wood, P.A., 1977. Controls of variation in suspended sediment concentration in the river Rother, West Sussex, England. Sedimentology 24, 437–445.